University of Stavanger

Faculty of Science and Technology

MASTER'S THESIS

Study program/ Specialization: Offshore Technology/ Subsea Technology	Spring semester, 2012 Open / ~~Restricted access~~
Writer: Whida Elastu Permana	..... (Writer's signature)

Faculty supervisor:
Prof. Arnfinn Nergaard, Ph.D.

External supervisor(s):

Title of thesis:
A Comparative Analysis of 21 inch and 16 inch Drilling Riser for Deepwater Application

Credits (ECTS):
30

Key words: Comparative, analysis, drilling, riser, deepwater.	Pages: 75 + enclosure: 19 pages + 1 CD Stavanger, June 14th, 2012 Date/year

Abstract

When offshore drilling needs to be conducted in deepwater and ultra-deepwater area, a significant increase of weight to be accommodated by the drilling rig due to more riser joints and larger drilling mud volume becomes a challenge that has to be carefully looked after. However, with the growing technology of semisubmersible drilling rigs, drilling systems and methods, subsea and downhole systems, and so on, the deepwater and ultra-deepwater drilling operation has been more enabled than ever. This is supported by the fact that the world record for drilling depth has exceeded 10000 ft (3048 m) today.

With more and more weight to be handled as the water depth goes deeper, and especially when heavy density drilling fluid needs to be used as well, drilling rig may arrive at a level where its capacities also need to be increased. Otherwise, it will not be adequate to fulfill the required parameters as stated by the regulating standards. A smart concept for drilling riser was then introduced with main objective to reduce the excessive weight resulted from deepwater application by replacing the conventional 21 inch diameter drilling riser with the slim 16 inch diameter drilling riser. As the weight and requirements related to this will be reduced, there is a possibility that the slim riser can be utilized further to even deeper water area without modifying existing capacities of the drilling rig, or even by using smaller capacity rigs.

Keywords: offshore, drilling, deepwater, riser, slim, rig.

Acknowledgement

This thesis is done to fulfill one of the compulsory requirements for completing master degree study in Offshore Technology at Faculty of Science and Technology, University of Stavanger, Norway. All related work, with respect to this thesis, was carried out for about five months starting from January until June 2012 in Stavanger.

In this opportunity I would like to specially thank my supervisor Prof. Arnfinn Nergaard, Ph.D. for all his advices, guidances, and efforts throughout the completion of this thesis, and Lasse Moldestad from Odfjell Drilling & Technology AS for his invaluable supports, assistances, explanations, and time for discussions whenever needed during the work.

I also want to express my sincere gratitude to both my parents Drs. Lashari, M.T. and Ratna Kusumastuti for their endless love and support during this 28+ years age of mine. I dedicate this thesis to them.

And last but not least, I want to thank my love Neng Rina Purnamasari for her patience, prayers, understandings, and encouragements that made me realize more than ever how important she is to me.

Stavanger, June 14th, 2012

Table of Contents

List of Figures

List of Tables

Chapter 1
Introduction

1.1 General

Offshore drilling vessel technology has been advancing to its more robust and reliable state since around 1960s. From a pioneer idea of floater concept using a converted barge as a simple submersible rig in shallow water area like swamps and creeks, the oil and gas industry has seen the transformation of the concept to the now so called semisubmersible mobile offshore drilling unit (MODU) which also has been developing from first generation until the latest sixth generation form today. There also exists several other type of drilling unit with as sophisticated technology as the semisubmersible such as drill ship, jack-up rig, and platform drilling rig with their advantage/disadvantage points and different specialities compared to each other.

The playing ground of the offshore drilling operation has also been expanding along with the progression of drilling vessel and drilling system technology. In the 1950's, the early period of offshore rotary drilling, wells were drilled at maximum water depth of no more than 100 m. The subsea production systems even had not been able to go this deep at that time since they were at least a decade behind to reach the same depth as the drilled well. In 2003, drilling have spectacularly reached to world record water depth of 3051 m achieved by Transocean (see Chapter 2). This tremendous drilling depth was just a little ahead of the achievement of the subsea production system so their technology can be said roughly to be at the same pace as of today.

In the mean time, subsea drilling system itself is also developing. In the early period of offshore drilling the system was known to commonly consist of two stack systems, large bore low pressure and smaller bore high pressure (Theiss, 2003). Subsea engineers then invented the single stack system full bore high

pressure and hence obsoleted the dual stack system with respect to practicality of operations and shorter required trip even though increase of the stack weight was also one of the unavoidable disadvantages.

Another significant invention is in the drilling and well design method. The technologies are for example dual gradient drilling, expandable tubulars, managed pressure drilling, slimhole drilling, and riserless mud return just to name a few. So, it is now enabled for drillers to use fewer casings to reach extreme target formation depth. This is of course very favourable for the industry as the lesser requirements to fulfill means also lesser costs to pay.

With all the advancing technologies in offshore drilling, subsea and drilling engineers are made able to be creative by having more options to solve all the previously unsolved problems using more efficient way to explore even deeper area than the present record, if possible, without sacrificing quality of the results.

1.2 Drilling riser system and the challenge

The conduit that connects the wellhead on the seabed to the vessel on the sea surface is called drilling riser or sometimes it is also called marine riser. The main purpose of this type of riser is, in brief, to provide a passage for downhole equipment such as drill bit and running tools to perform their designated job, and also not less important is to circulate the drilling mud back from the drilled well to the surface. Because of this reason, drilling riser has important role in offshore drilling operation.

The riser system itself is generally built from series of large diameter main pipes with smaller pipes attached to it on the outside which is referred as choke and kill lines used for well control purpose (Maclachlan, 1987). At upper part of the riser system a slip joint is installed to compensate the effect of heave/vertical movements of the vessel to the riser tension. Slip joint, sometimes also called telescopic joint, normally consists of an inner and outer barrel where the inner barrel can “slip” into the outer barrel at some limited length.

In deepwater drilling, flexible joints are often to be found in the drilling riser system installed at top and bottom of the riser and often called as the upper and lower flex/ball joint. The flexible joint allows some limited rotation angle at the riser connection so it has an important main purpose to reduce the stress in the riser pipe induced by the offset/horizontal movements of the vessel, due to existence of some rotational stiffness, compared to if the connection was designed to be very stiff or fixed.

The weight of the whole riser system must be supported by the vessel by means of tensioning device. The tension force provided by the tensioning device should be at least enough to accommodate the dead weight of the riser pipe, the content (drilling fluid), the environmental forces, and also taking account for the resulted buoyancy force exerted by the sea. The tensioning device should be reliable to provide the required tension so it will minimize the chance of damaging the riser during drilling activity or the chance of lack of required tension for disconnection/abandonment operation. General illustration of drilling riser components can be seen in Figure 1.

In the conventional system, the riser used for the drilling operation is the popular 21 inch nominal outer diameter pipe to be used with $18\frac{3}{4}$ inch full bore blow out preventor (BOP) stack. Using pipe this large, it allows more casing strings (with different diameter) to be installed inside the drilled hole below the stack so well designers have more options to set in casings especially in the situation of wildcat drilling.

However, as the water depth goes deeper the required tension increases since the overall riser length to be supported by the tensioning device becomes longer. This condition affects the volume of the content (drilling fluid) that needs to be taken care both in the tension and storage space requirement onboard the rig. This depth vs. size relationship seems to give engineers no choice but to keep increasing the sizes of each required components every time conducting deeper exploration.

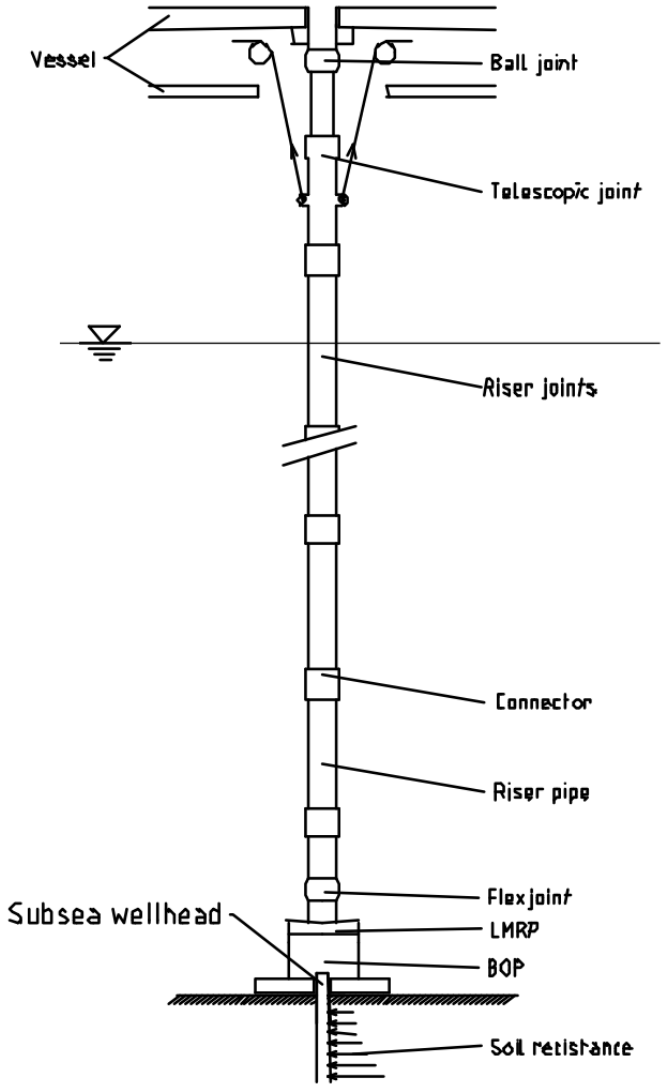

Figure 1. Drilling riser components (DNV, 2010).

An interesting concept emerged, not to break the relationship above, but to give engineers more options to conduct drilling operation in areas deeper than before. It is basically a derivative of the conventional system since it adopts the principle of conventional method only now the difference is by using smaller, slim 16 inch nominal diameter pipe instead of 21 inch.

Because of the reduction in riser size, it should be understood already the advantages that can be obtained. It is true that the slim riser diameter will then obviously limit the casing sizes that can be run inside, but some techniques have even been found as well to overcome this if well design requires some larger

casing diameters to be installed below the stack. Quick comparison of the differences resulted from application of these two riser concepts were found from a paper by Taylor, et al. (2003) and can be seen in the following Table 1 and 2 for illustration purpose.

Riser Diameter (in)	Water Depth (ft)	Riser Dry Weight (kips)	Riser Mud Volume (bbls)	Mud Weight in Riser (kips)		
				12 ppg	15 ppg	17 ppg
21	1500	940	583	293.5	367	416
21	10000	6267	3886	1958	2448	2774
16	10000	4000	2040	1028	1285	1457

Table 1. Weight characteristics for different riser sizes (Taylor, et al., 2003).

Rig Specification Item	Riser Diameter		Changes
	21 inch	16 inch	
Variable deck load (long tons)	7000	5500	-21%
Hoisting capacity (long tons)	1000	750	-25%
Tensioning capacity (kips)	3000	1750	-42%
Mud pit capacity (bbls)	5200	3500	-33%
Mud pump capacity (HP)	6000	4800	-20%
Riser racks (sq.ft)	9000	5500	-39%
Hull displacement (long tons)	50000	35000	-30%
Hull steel (long tons)	16000	10000	-28%
Total building cost ($ million)	300	180	-40%

Table 2. Rig comparison for different riser size (Taylor, et al., 2003).

1.3 Objective and limitation

A case of 21 inch conventional drilling riser in operation at approximately 3000 m water depth will be analyzed using a latest (sixth) generation semisubmersible rig with maximum drilling fluid to be used is 17 ppg (which is approximately equal to 2.0 specific gravity of seawater). The riser will be designed accordingly to be capable to do the job. The tension capacity of the sixth generation rig will have to hold the enormous required top tension for keeping the 21 inch riser in operation and satisfying all the design criteria as recommended by the regulating codes.

Another case which is almost similar but now using 16 inch slim drilling riser instead will also be analyzed with same 17 ppg drilling mud to be applied to the riser to have an “apple to apple” comparison with the previous conventional 21 inch drilling riser analysis case. This slim riser will also be designed to satisfy the burst requirements for the heaviest 17 ppg mud inside and for this case it can be understood immediately that the required top tension will be obviously reduced and hence the required tensioner capacity of the rig to be used for operation does not need to be as high as for the case of 21 inch riser.

This immediate fact is actually in analogy with using a smaller or older generation rig to operate instead of the more costly daily-rated latest generation rig for case of slim riser application. A design water depth will be obtained for application of this 16 inch slim riser where all requirements and criteria from the codes are still need to be fulfilled as well.

A fully 3-dimensional finite element computer software Orcaflex will be utilized for the required analysis. Subsea equipments (i.e. blow out preventor stack, wellhead assembly, etc.) and well/casing design criticality requirements will not be taken into account and considered to just enable this slim riser concept to be conducted to limit the report from the need of broader analysis. Downhole technologies such as dual gradient drilling, expandable tubulars, managed pressure drilling and the other enabling technologies for application of this slim 16 inch riser concept are the root basis for the needs of this riser analysis but they are out of scope of this report and will not be discussed in more detail.

1.4 Structure of report

This report consists of nine chapters. Brief overview of offshore drilling technology, quick descriptions on author's main interest which is the drilling riser and the challenge that arises, and also what becomes the main objective of this report including its limitations are found already in this chapter.

Chapter 2 describes the state of the art of semisubmersible drilling rig, the transformation that has been happening during its fifty years of existence from the oldest generation until the latest generation today.

Chapter 3 gives brief review of fundamental theory, including the beam small deflections theory, buoyancy and effective tension principle, hydrodynamic force, wave theory, theory of dynamics of structures, and the circumferential stress due to pressure on pipes.

Chapter 4 provides the design criteria for drilling riser analysis. Three most recognized international standards for drilling riser are described here, they are the DNV-OS-F201 Dynamic Risers, API RP 16Q Design, Selection, Operation, and Maintenance of Marine Drilling Riser Systems, and ISO 13624-1 Part 1: Design and operation of marine drilling riser equipment.

Chapter 5 provides the brief overview about the Orcaflex software which is used for analysis. Main points for description are about its coordinate systems, the discretized line model, equation of motion, and reference for stress calculation.

Chapter 6 describes the methodology for the analysis. There can be found separately the proposed configuration for the conventional 21 inch drilling riser and the slim 16 inch drilling riser. Environmental conditions as well as other considerations such as tensioner midstroke and vessel offsets are explained there.

Chapter 7 provides the analysis result and the discussion.

Chapter 8 gives the conclusion.

Chapter 9 suggests the recommendation for future work to be conducted.

Chapter 2
State of the Art of Semisubmersible Drilling Rig

Offshore drilling rig has transformed several times and each of the transformation marks an achievement in the world of drilling technology. There is no exact guideline about division classification for semisubmersible drilling rigs, however, they are generally grouped according to the year they were built and also the water depth capability.

The first semisubmersible drilling rig was the Bluewater I built by Shell Oil and was operating in the 1960s. This rig consisted of four columns and set as the first generation of drilling rig with water depth capability less than 600 ft (182 m). The bright prospect of semisubmersible technology was immediately followed since then by other first and second generations rigs in the 1970s with water depth capability about 1000 ft (305 m).

Another world achievement occured in the second generation era with the introduction of the world first self-propelled semisubmersible Ocean Prospector rig built by Odeco (now Diamond Offshore) in 1971 (Offshore Energy Center, 2000). This rig consisted of twelve columns with two main tubular hulls and rated for water depth up to 1700 ft (518 m) (SEC Info Database, 2002).

The Ocean Prospector was a successful semisubmersible rig that set example for several later rigs as a basis for design. Today, most of those early generation semisubmersibles have been retired and cold-sacked from service. The latest information obtained for the Ocean Prospector rig is that after nearly 14 years it got decommissioned and left idle in a cruise harbor in Texas since 1998, it is now under repairments and modifications at a shipyard to be sent out to work on offshore oil fields again in the future (Oil Price, 2012).

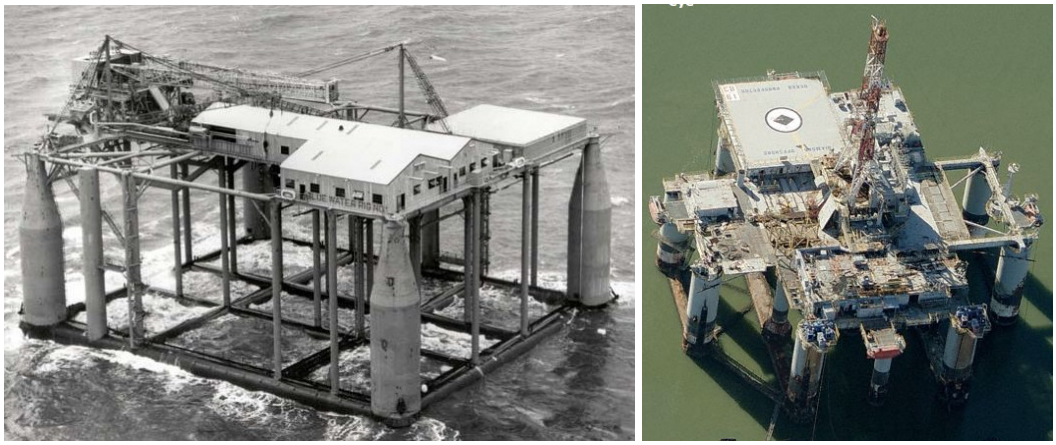

Figure 2. Left to right: Bluewater I and Ocean Prospector rig (Wikipedia and Virtual Globe Trotting, 2012).

The third generation of semisubmersible drilling rig started to set new record of water depth capability up to 1500 m (4921 ft). This era began in around early 1980s. Some examples of semisubmersible rig in this generation are Atwood Oceanics' Atwood Falcon, Odfjell Drilling's Deepsea Bergen, Petrobras' Petrobras X, Transocean's GSF Arctic I (ex Global Marine Santa Fe), and so on. The third generation semisubmersible rigs were originally having tensioner capacity with range 640-960 kips (290-435 ton). Most of those third generation drilling rigs had been refurbished and/or upgraded to newer generation with higher specifications in the 1990s as the demand for harsh environment drilling rigs with water depth capability 1500-5000 ft (457-1524 m) was higher than the supply.

During 1996-1998 alone there were 30 semisubmersible upgrades (either from second or third generation) done to fulfill market's demand (Offshore Magazine, 2001). The decision for upgrade was also based on insufficient time availability for new construction since the competition was tight. The upgrade generally focused on stability enhancements such as increasing the variable deck load (VDL) of the rig so that it could carry more weights onboard as the water depth capability was going to be shifted up, mud system enhancements such as expanding the mud pit capacity, subsea and drilling equipments enhancements such as replacing the older-lower pressure subsea manifolds, mooring system upgrades, and other miscellaneous upgrades such as for space and storage.

The 1990s was the modernization era where many rig modifications and upgrades were done (see Table 3) resulting in more powerful rig specification which was then referred as the fourth generation of semisubmersible rig. However, the first ever built semisubmersible rig of this generation was the Transocean's Polar Pioneer back in 1985 (Transocean Beacon Magazine, 2011). The world record water depth capability for this fourth generation was around 7000 ft (2133 m) recorded in the mid 1980s and went up to average of 7500 ft (2286 m) in the mid 1990s (Mustang Engineering, 2011).

Rig Manager	Rig Name	Year Built	Year Upgraded	Generation
Diamond Offshore	Ocean Quest	1973	1996	2/4
Diamond Offshore	Ocean Winner	1976	1996	2/3
Odfjell Drilling	Deepsea Trym	1976	1996	2
Pride International	South Seas Driller	1977	1996	2
R&B Falcon	J.W. McLean	1974	1996	2
Atwood Oceanics	Atwood Southern Cross	1976	1997	2
Atwood Oceanics	Atwood Hunter	1981	1997	2/3
Diamond Offshore	Ocean Star	1973	1997	2/4
Diamond Offshore	Ocean Victory	1972	1997	2/4
Diamond Offshore	Ocean Yorktown	1976	1997	2/3
Dolphin Drilling	Borgny Dolphin	1977	1997	2
Dolphin Drilling	Bredford Dolphin	1980	1997	2/3
Global Marine	Glomar Arctic I	1983	1997	3
Pride International	Nymphea	1982	1997	3
Petrobras	Petrobras XVII	1984	1997	2
Transocean Sedco Forex	Sedco 707	1976	1997	2/4
Transocean Sedco Forex	Transocean 97	1977	1997	2
Transocean Sedco Forex	Transocean 96	1975	1997	2
Transocean Sedco Forex	Transocean Amirante	1981	1997	2/3
Atwood Oceanics	Atwood Falcon	1983	1998	3
Caspian Drilling	Istiglaliyet	1993	1998	2
Caspian Drilling	Dada Gorgud	1980	1996 & 1998	2
COSDC	Nanhai V	1983	1998	3
CROSCO	Zagreb I	1977	1998	2
Dolphin Drilling	Bideford Dolphin	1975	1998	2/4
Japan Drilling	HAKURYU-3	1974	1998	2
Petrobras	Petrobras X	1982	1998	3
Petrobras	Petrobras XXIII	1985	1998	3/4
R&B Falcon	Falcon 100	1974	1998	2
Tor Drilling	Tor Viking	1973	1998	2
Odfjell Drilling	Deepsea Bergen	1983	1996 & 1999	3
Diamond Offshore	Ocean Concord	1975	1999	2
Diamond Offshore	Ocean General	1976	1999	2
Noble Drilling	Noble Homer Ferrington	1985	1999	2/4
Industrial Perforadora de Campeche	La Muralla	1989	2000	2

Table 3. Semisubmersibles upgraded in mid 1990s (Offshore Magazine, 2001).

Other examples of semisubmersible rig belong to this fourth generation are Seadrill's West Alpha, Diamond Offshore's Ocean Valiant, Saipem's Scarabeo 5, and so on. In this era, the majority of the semisubmersible drilling rigs, including those from older generation after being upgraded, have tensioner capacity with range around 960-1920 kips (435-871 ton).

The 2000s was the period where fifth generation semisubmersible rigs showed their domination in the drilling industry. Many claimed to be the first company who delivered the first fifth generation semisubmersible rig, for example Ocean Rig with their Leiv Eiriksson and Eirik Raude (Euro Asia Energy, 2009), Smedvig with their West Future II (Yokokura, et al., 1998), and Transocean with their Sedco Express, Sedco Energy, and Cajun Express rigs (Transocean, 2012). Another notable semisubmersible rig in this period is the Smedvig's West Venture which was regarded as the world's first fifth generation DP (dynamic positioning) drilling rig (ABB Marine, 2012).

During this fifth generation rig era, average water depth reach for drilling went up beyond 9000 ft (2743 m). The famous record for this was the 3051 m (10011 ft) DP drilling water depth achievement in the Gulf of Mexico at Toledo well by Transocean's Discoverer Deep Seas in 2003 (see Figure 3). In general, the majority of fifth generation semisubmersible drilling rigs have water depth capability of 7500-10000 ft (2286-3048 m) and tensioner capacity with range 960-3200 kips (435-1452 ton). Figure 3 shows the worldwide progression chart of water depth capabilities for offshore drilling and production until year 2011.

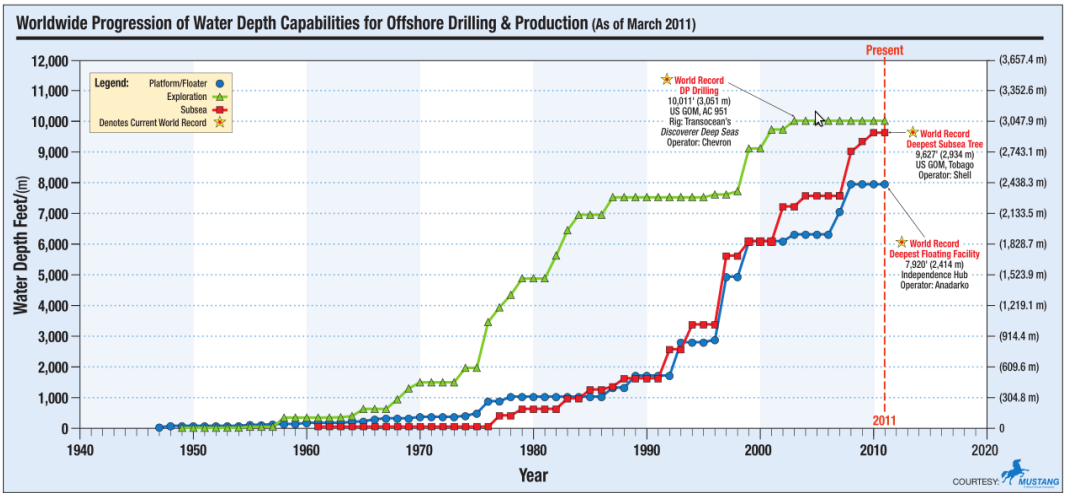

Figure 3. Water depth capability progression (Mustang Engineering, 2011).

While the drilling industry was excited by the 3051 m water depth achievement, Aker ASA initiated a project to build the next generation of semisubmersible rig (sixth) called the Aker H-6e in 2005 (World Oil, 2005). The first two rigs were delivered in 2009 and now owned by Transocean as Transocean Spitsbergen and Transocean Barents, after they completed the 100% share acquisition of Aker Drilling ASA in 2011.

Since then, many other sixth generation rigs were built to fulfill the market's demand of excellent motion characteristics drilling rig to operate in extreme and harsh environment area. More examples for the sixth generation rig are Odfjell's Deepsea Atlantic and Deepsea Stavanger, CNOOC's Hay Yang Shi You 981, Seadrill's West Aquarius, Noble's Clyde Boudreaux, and so on. The sixth generation drilling rigs generally have water depth capability of at least 10000 ft (3048 m) and tensioner capacity with range 1920-3200 kips (871-1452 ton).

Being in the latest and most advanced sixth generation, day rate of these rigs soars as the tightness rig availability increases. It is known already that for a 7500 ft (2286 m) rated semisubmersible the day rate was priced at $500,000 (E&P Magazine, 2011). For more advanced ultra deepwater rigs the day rate has breached that half million dollar threshold and is expected to exceed $600,000 by midyear 2012 (E&P Magazine, 2012).

The rapidly fading visibility of ultra deepwater rig availability was one of the reason for operators to set a long term contract with rig owners. Because of this and from the trend in Figure 4 there is high chance that the industry may see more rig upgrades and newly constructed rigs and even probably the very first seventh generation rig coming in the near future.

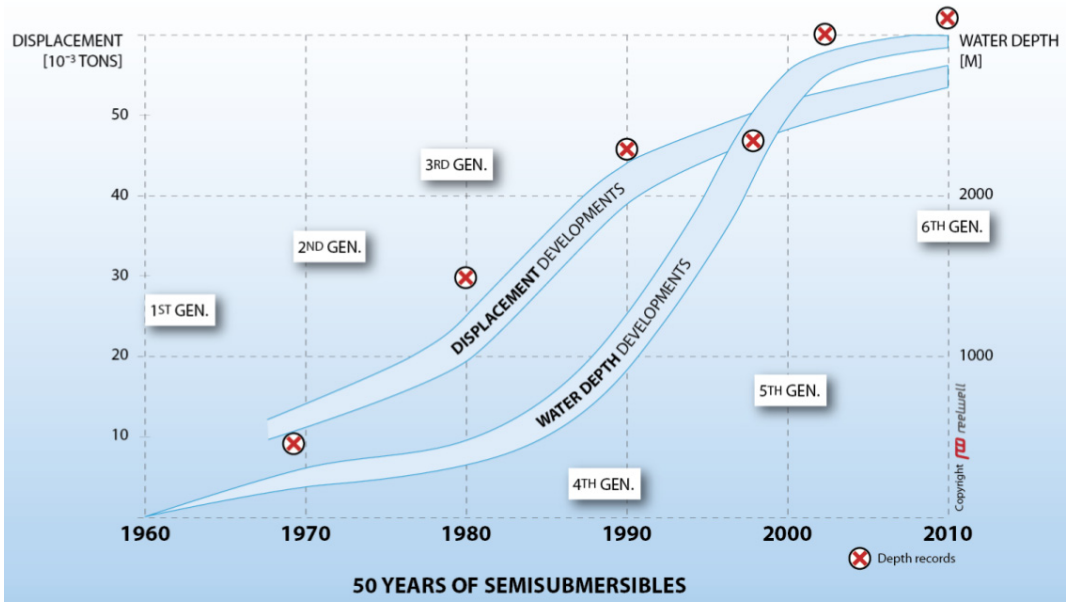

Figure 4. Fifty years of semisubmersibles (Nergaard, 2012).

Chapter 3
Review of Fundamental Theory

3.1 Bending and small-angle deflection theory

Drilling riser is basically a tensioned beam having small angle deflection generally less than 10 degrees (measured from vertical in this case). Because of this condition, the fundamental beam small angle deflection theory can describe the drilling riser differential response equation very well. It will be described here briefly the theoretical background for the beam deflection before developing the general governing equations for drilling riser.

This subchapter refers to Case, et al. (1999) and Sparks (2007). Consider a beam in its initial and under pure bending form in Figure 5. Famous assumption for pure bending theory is that plane cross section remains plane and normal to its longitudinal fiber after bending. In this case, fiber AF will be under tension and stretched and fiber BD will be compressed while in the mean time the neutral axis fiber δz will remain unchanged.

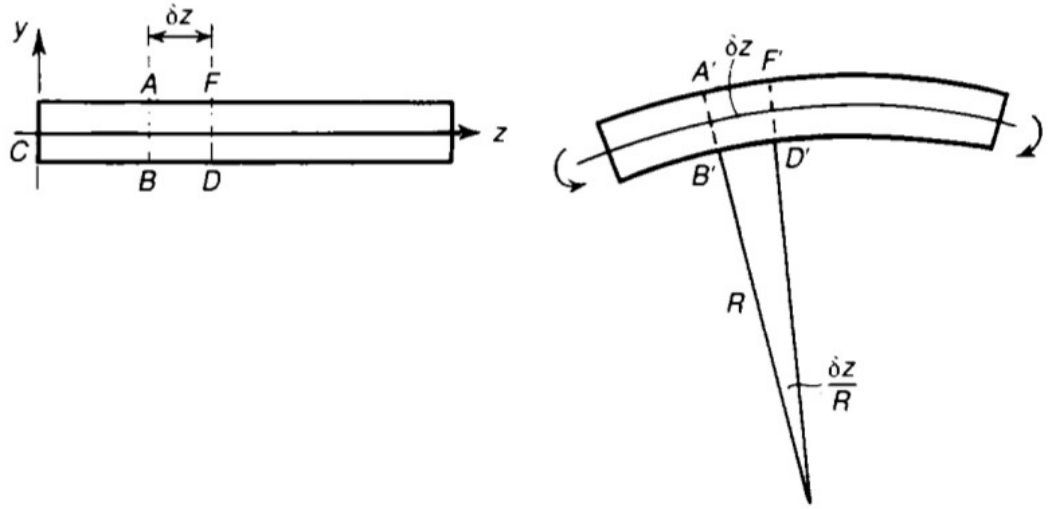

Figure 5. Initial and bent form of a beam in pure bending (Case, et al., 1999).

Further assumption to be added is that the beam is a linearly elastic material, hence it follows Hooke's law. For small angle $\delta z / R$ this condition leads to the well known stress-strain equation (see Figure 6 for reference):

$$\varepsilon = \frac{H'J' - HJ}{HJ} = \frac{(R+y) - R}{R} = \frac{y}{R} \tag{3-1}$$

$$\sigma = E\varepsilon = \frac{Ey}{R} \tag{3-2}$$

where

ε = strain

σ = stress

R = radius of curvature

E = Young's modulus of elasticity

Bending moment at the cross section can be obtained by integrating bending stress over the cross section area multiplied by the distance to the neutral axis. Note that above the neutral axis there is tensile stress and below there is compressive stress in this particular case, so the moment about x axis will be combination of them. The integration result is given by:

$$M = \int^{A} \sigma y dA = \frac{Eb}{R} \int^{h} y^2 dy = \frac{EI_x}{R} \tag{3-3}$$

where

M = bending moment about x axis

h = height of beam cross section

b = width of beam cross section

I_x = moment of inertia about x axis = $\frac{bh^3}{12}$

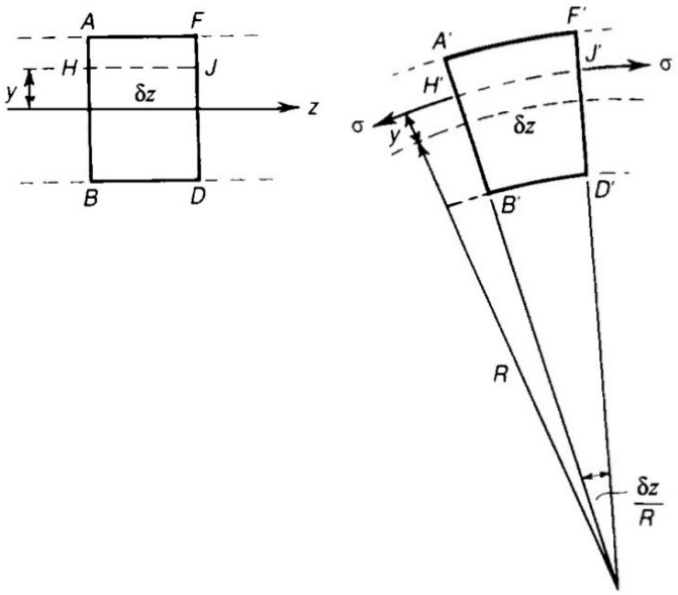

Figure 6. Bent element of a beam (Case, et al., 1999).

From equation (3-3) it can be obtained the relationship between curvature and bending moment for linearly elastic material as:

$$\frac{1}{R} = \frac{M}{EI} \tag{3-4}$$

The curvature from equation (3-4) above can also be written in relation with deflection curve. Figure 7 shows that if the deflection slope θ is $\delta y / \delta z$ then for small angle $\delta\theta = \delta z / R$ the curvature becomes:

$$\frac{1}{R} = \frac{\delta\theta}{\delta z} = \frac{\delta}{\delta z}\left(\frac{\delta y}{\delta z}\right) = \frac{\delta^2 y}{\delta z^2} \tag{3-5}$$

where

$\frac{1}{R}$ = curvature

$\frac{\delta\theta}{\delta z}$ = rate of change of slope θ with respect to z

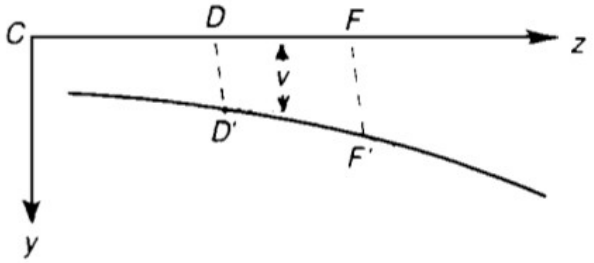

Figure 7. Displacement of beam longitudinal axis (Case, et al., 1999).

So it can now be understood the relationship between curvature, deflection, and bending moment of a beam from equation (3-3) and (3-5) including the sign convention for bending moment which is positive for sagging:

$$EI\frac{\delta^2 y}{\delta z^2} = -M \tag{3-6}$$

By having the fundamental deflection formula, now consider a near vertical segment of a beam with forces acting on it as shown in Figure 8. With length of the segment is δx and near vertical angle is dy/dx then the sum of forces in horizontal direction is:

$$\delta F + \delta\left(T\frac{dy}{dx}\right) + f(x)\delta x = 0 \tag{3-7}$$

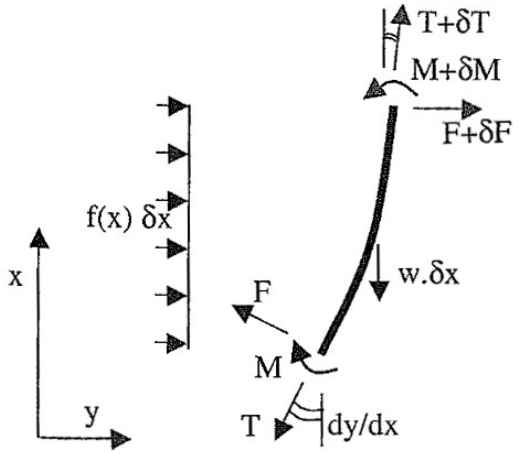

Figure 8. Forces acting on a tensioned beam segment (Sparks, 2007).

Since shear force F is basically the rate of change of moment dM/dx then from equation (3-7) it can be derived:

$$\frac{dF}{dx} + \frac{d}{dx}\left(T\frac{dy}{dx}\right) + f(x) = 0 \qquad (3\text{-}8)$$

$$\frac{d^2M}{dx^2} + \frac{d}{dx}\left(T\frac{dy}{dx}\right) + f(x) = 0 \qquad (3\text{-}9)$$

Knowing that for near vertical beam dT/dx equals w (the weight per unit length), hence for linearly elastic material with constant bending stiffness EI the equation (3-9) can be rewritten as:

$$EI\frac{d^4y}{dx^4} - T\frac{d^2y}{dx^2} - w\frac{dy}{dx} - f(x) = 0 \qquad (3\text{-}10)$$

Equation (3-10) above is a fourth order differential equation that shall govern the deflection and curvature of near vertical beam segment under tension T and external lateral force $f(x)$. In case of submerged beam, T to be referred as the effective tension and w is the apparent weight. Concept of effective tension and apparent weight will be discussed more in following Subchapter 3.2.

3.2 Concept of buoyancy and effective tension

Archimedes' law states that any submerged body, either fully or partially, will receive an upward force which equals to the weight of the displaced fluid where it is submerged into. This upward force is well known as buoyancy force. It is because of the buoyancy force that the body seems less heavy when a weighing scale is attached to it and two measurements are taken e.g. before and after the submersion.

The pressure field on the body is the same pressure field which acts on the displaced fluid which has resultant as upward buoyancy force but at the same time it is equalized by the weight of the displaced fluid itself. So, the submerged weight of the body equals to its in-air weight subtracted by the weight of the

displaced fluid W_f (see Figure 9). The submerged weight of a body is often called as the apparent weight W_{app} .

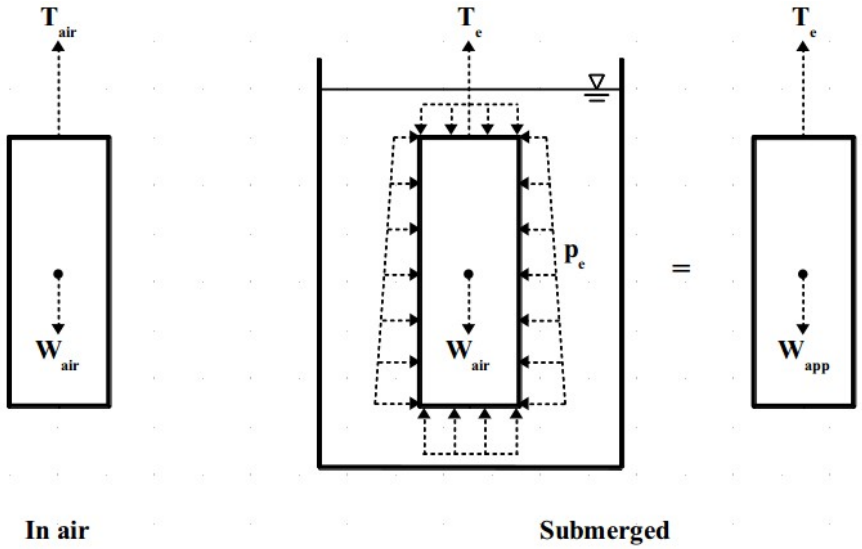

Figure 9. Concept of buoyancy.

Once the basic buoyancy concept above is understood, it can now be used to find the distribution of tension along the length of the body. Since the pressure field on a body of displaced fluid and the weight of the displaced fluid itself will always be in equilibrium they are "exchangeable" to each other and this will be helpful for case of irregular shaped bodies where the horizontal pressure effect can not be quickly taken as eliminating each other anymore. The horizontal pressure field can be seen is identical so they will neglect each other. Since the body is in equilibrium with A_e as the constant outer cross section area it can be written:

$$T_e = W_{app} = W_{air} - W_f = W_{air} - A_e \Sigma p_e \tag{3-11}$$

From free body diagram of the submerged body in Figure 10, tension distribution can then be derived as:

$$T_e(x) = T_e - W_{air}(x) + A_e \Sigma p_e(x) \tag{3-12}$$

$$T_e(x) = T_e - W_{air}(x) + A_e\left(p_e(x) - p_e(x=0)\right) \tag{3-13}$$

Since top tension T_e and $A_e p_e(x=0)$ are constant then equation (3-13) above can be rewritten in simpler from as:

$$T_e(x) = T_{tw}(x) + A_e p_e(x) \tag{3-14}$$

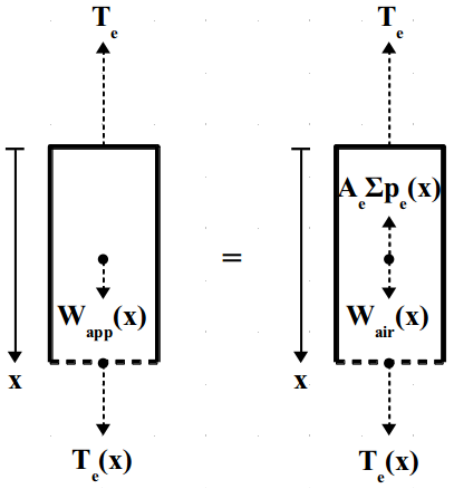

Figure 10. Submerged free body diagram.

In equation (3-14) a new variable T_{tw} is introduced and referred as the true wall tension while in the same time T_e is the effective tension. Reversed free body diagram (e.g. x starts from bottom) will give the same result. Similar approach can be employed for the case when the body is also subject to internal hydrostatic pressure with constant inner cross section area A_i. From Figure 11:

$$T_e(x) = T_e - W_{air}(x) - A_i \Sigma p_i(x) + A_e \Sigma p_e(x) \tag{3-15}$$

$$T_e(x) = T_e - W_{air}(x) - A_i\left(p_i(x) - p_i(x=0)\right) + A_e\left(p_e(x) - p_e(x=0)\right) \tag{3-16}$$

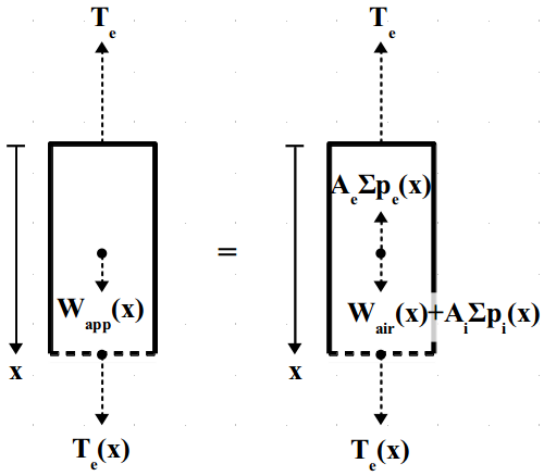

Figure 11. Submerged free body diagram with internal hydrostatic pressure.

Again by knowing that T_e, $A_e p_e(x=0)$, and $A_i p_i(x=0)$ are constant, previous equation (3-16) can then be rewritten equivalently as:

$$T_e(x) = T_{tw}(x) - A_i p_i(x) + A_e p_e(x) \tag{3-17}$$

Equation (3-17) above is the general form of effective tension equation. It can be seen that it will be less complicated to find the effective tension first then after that the true wall tension. The true wall tension is often referred just as wall tension.

3.3 Hydrodynamic forces

Hydrodynamic forces on structures are normally calculated using the well known Morison's equation/postulate that he derived when studying about wave-induced hydrodynamic forces on vertical piles (Morison, et al., 1950). This equation describes the force as a combination of drag and inertia force components. Hydrodynamic forces per unit length acting on a submerged fixed cylinder as function of depth and time are given by:

$$f = f_D + f_M \tag{3-18}$$

$$f(z,t) = \frac{1}{2} C_D \rho D u(z,t) |u(z,t)| + C_M \rho \frac{\pi D^2}{4} \dot{u}(z,t) \tag{3-19}$$

where

C_D = drag coefficient

ρ = water density

D = cylinder diameter

C_M = inertia coefficient

u = horizontal water particle velocity

$\dot{u}$ = horizontal water particle acceleration

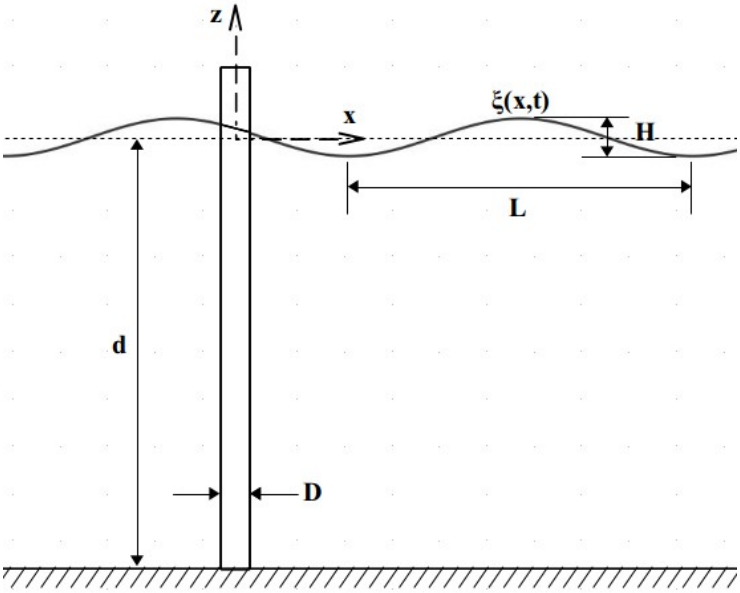

Figure 12. Submerged fixed cylinder exposed to wave.

Total maximum force on cylinder body can be obtained by integrating equation (3-19) with respect to z as follow:

$$F(t) = \int_{-d}^{\xi(t)} \{f_D(z,t) + f_M(z,t)\} dz \tag{3-20}$$

$$F_{max}(t) = \int_{-d}^{\xi(t)} f_D(z,t) dz + \int_{-d}^{0} f_M(z,t) dz \tag{3-21}$$

Equation (3-21) is written by knowing that between water particle horizontal velocity u and acceleration $\dot{u}$, which compose the drag and inertia force, there is 90^o phase difference so their upper integration limits are different with purpose to get their maximum values.

Combination with existence of current is possible and this will add more drag force on the structure due to current speed u_c. For the case of cylinder which is also moving laterally in the same direction as the flow, equation (3-19) to be modified as (Sparks, 2007):

$$f = \frac{1}{2} C_D \rho D (u - v)|(u - v)| + C_M \rho \frac{\pi D^2}{4} \dot{u} - (C_M - 1) \rho \frac{\pi D^2}{4} \dot{v} \tag{3-22}$$

where

v = cylinder velocity

$\dot{v}$ = cylinder acceleration

Drag coefficient C_D for circular cylinder is a dimensionless parameter which depends on Reynolds number Re, Keulegan-Carpenter number KC, and surface roughness. Drag and inertia coefficient C_M should preferably be obtained from full scale model testing while on the other hand it is difficult to perform. The inertia coefficient has theoretical value of 2.0 based on potential flow theory and it is common design practice to use that theoretical value (Almar-Næss, 1985). The $(C_M - 1)$ coefficient in equation (3-22) above is often referred as the added mass coefficent.

However, the use of hydrodynamic force formulas above has limitations in their area of application. Some of the limitations are (Gudmestad, 2011):

1. Non-breaking wave

   The equation is for regular waves. However, any irregular wave can be written as summation of regular waves. Wave breaking criteria for regular wave is:

   $$\frac{H}{L} \geq 0.14$$

   where

   H = wave height

   L = wavelength

2. The wave acceleration is considered relatively constant over the diameter of the structure otherwise reflection of the incoming wave will occur which is often called as wave diffraction. The criteria for this is that the structure is slender enough compare to the wave length $\frac{D}{L} \leq 0.2$.

Until today, Morison's equation is still considered to give the most accurate wave forces on cylindrical structure even though it was first derived more than sixty years ago. Selection of wave theory to be used in the equation is important and

has become one of the key discussions as linear and higher order nonlinear theories are both available (for further reference see Sarpkaya and Isaacson, 1981).

3.4 Waves

Ocean wave is irregular since it is composed of many waves component which every single of them has their own wave height and period. This wave component is called regular wave. Regular wave is a periodic sinusoidal wave that can be identically divided by length into one individual wave form. The simplest theory that describes this wave form is the linear wave theory which is also referred as Airy's wave theory. In brief, this wave theory was derived based on existence of scalar function Φ as the velocity potential which satisfies the assumptions of continuity of mass flow and incompressible fluid $\nabla^2\Phi = 0$ (Dean and Dalrymple, 1991).

By using boundary conditions, the potential gives the 3-dimensional wave profile and kinematic properties as follow:

$$\Phi(z,x,t) = \frac{\xi_o g}{\omega}\frac{\cosh k(z+d)}{\cosh kd}\cos(\omega t - kx) \tag{3-23}$$

Surface profile $(z=0)$:

$$\xi(x,t) = -\frac{1}{g}\frac{\partial \Phi}{\partial t} = \xi_o \sin(\omega t - kx) \tag{3-24}$$

Horizontal and vertical water particle velocity:

$$u(z,x,t) = \frac{\partial \Phi}{\partial x} = \frac{\xi_o g k}{\omega}\frac{\cosh k(z+d)}{\cosh kd}\sin(\omega t - kx) \tag{3-25}$$

$$w(z,x,t) = \frac{\partial \Phi}{\partial z} = \frac{\xi_o g k}{\omega}\frac{\sinh k(z+d)}{\cosh kd}\cos(\omega t - kx) \tag{3-26}$$

Horizontal and vertical water particle acceleration:

$$\dot{u}(z,x,t) = \frac{\partial u}{\partial t} = \xi_o g k \frac{\cosh k(z+d)}{\cosh kd}\cos(\omega t - kx) \tag{3-27}$$

$$\dot{w}(z,x,t) = \frac{\partial w}{\partial t} = \xi_o g k \frac{\cosh k(z+d)}{\cosh kd}\sin(\omega t - kx) \tag{3-28}$$

where

Φ = velocity potential

ξ_o = wave height

g = gravitational acceleration

k = wave number

d = water depth

ω = angular frequency

The wave number k equals to $2\pi/L$ and can be related to angular frequency ω using the so called dispersion relationship $\omega^2 = gk \cdot \tanh kd$. It can be seen that as kd increases with water depth, the hyperbolic function ratio $\cosh k(z+d)/\cosh kd$ and $\sinh k(z+d)/\cosh kd$ in equation (3-25) to (3-28) above will both converge to e^{kz}. This gives the exponential dissipation of wave particle velocity and acceleration as the water depth goes deeper.

However as described before, real ocean wave is irregular hence it will not have the same characteristics as the regular wave. Recorded wave time series/histories are analyzed to get the statistical properties of interest such as zero upcrossing period T_z (i.e. the average time between successive upcrossings at still water level) and significant wave height H_s (i.e. the average of one-third largest wave heights where each height is measured as the difference between the lowest trough and the highest crest in each upcrossing period). The process of describing irregular waves by its statistical properties is called stochastic process.

A wave spectrum $S(\omega)$ is constructed to define the energy of the sea surface using the statistical parameters obtained previously. Several spectral methods are available but the most often and commonly used in North Sea region are the Pierson-Moskowitz spectrum and the JONSWAP spectrum (Almar-Næss, 1985). Their formulations are as follow:

The Pierson-Moskowitz spectrum:

$$S(\omega) = {H_s}^2 T_z \frac{1}{8\pi^2}\left(\frac{\omega T_z}{2\pi}\right)^{-5} e^{\left(-\frac{1}{\pi}\left(\frac{\omega T_z}{2\pi}\right)^{-4}\right)} \tag{3-29}$$

The JONSWAP spectrum:

$$S(\omega) = ag^2\omega^{-5} e^{\left(-\frac{5}{4}\left(\frac{\omega}{\omega_p}\right)^{-4}\right)} \gamma^{e^{\frac{\left(\frac{\omega}{\omega_p}-1\right)^2}{2\omega^2}}} \tag{3-30}$$

The parameters a, ω_p (corresponding frequency when the spectrum is at its peak), and γ (the peakedness parameter) are dependent variable of H_s and T_z. Their values can be found in Table 4. The Pierson-Moskowitz spectrum is suitable for fully developed sea condition where wave growth is not limited by the size of area where it was generated and the wind blows over a long period of time in long fetch/distance. In contrary, the JONSWAP spectrum is applicable to condition where wave growth is limited by the size of generation area.

Wave spectrums will be considered to follow Rayleigh distribution if their spectral width parameter is close to zero (i.e. narrow-banded spectrum). In narrow-banded spectrum the wave time series are relatively regular where in broad-banded spectrum the time series are more random. Rayleigh distribution (spectral width parameter equals zero) is often to be chosen due to its simplicity in formulation. Some formulations according to this distribution are:
The zero order moment (i.e. total energy of the spectrum) is given by:

$$m_0 = \int_0^\infty \omega^0 S(\omega) d\omega \tag{3-31}$$

Significant wave height and zero upcrossing period can be calculated as:

$$H_s = 4\sqrt{m_0} = H_0 \tag{3-32}$$

$$T_z = 2\pi\sqrt{\frac{m_0}{m_2}} = T_{0,2} \tag{3-33}$$

T_{o2} (s)	Significant wave height (m) H_S (m)																								
	2.0-2.49	2.5-2.99	3.0-3.49	3.5-3.99	4.0-4.49	4.5-4.99	5.0-5.49	5.5-5.99	6.0-6.49	6.5-6.99	7.0-7.49	7.5-7.99	8.0-8.49	8.5-8.99	9.0-9.49	9.5-9.99	10.0-10.49	10.5-10.99	11.0-11.49	11.5-11.99	12.0-12.49	12.5-12.99	13.0-13.49	13.5-13.99	14.0-14.49	14.5-14.99
4.0-4.99	5.490 0.0138 0.1800	5.970 0.0201 0.1810	6.330 0.0277 0.1820	6.600 0.0359 0.1830	6.890 0.0485 0.1850																				
5.0-5.99	4.130 0.0064 0.1440	4.910 0.0094 0.1460	5.400 0.0129 0.1470	5.770 0.0171 0.1480	6.070 0.0219 0.1490	6.290 0.0267 0.1490	6.490 0.0323 0.1490	6.680 0.0390 0.1500	6.830 0.0455 0.1500	6.960 0.0523 0.1500															
6.0-6.99	1.260 0.0036 0.1110	3.370 0.0051 0.1200	4.280 0.0069 0.1220	4.860 0.0092 0.1240	5.210 0.0113 0.1240	5.530 0.0142 0.1250	5.770 0.0170 0.1250	5.840 0.0180 0.1260	6.170 0.0239 0.1260	6.320 0.0274 0.1260	6.490 0.0323 0.1270	6.610 0.0363 0.1270	6.730 0.0410 0.1270	6.870 0.0475 0.1280	6.960 0.0523 0.1280										
7.0-7.99		1.090 0.0032 0.0960	1.650 0.0042 0.0980	3.620 0.0055 0.1050	4.240 0.0067 0.1060	4.690 0.0083 0.1070	5.040 0.0102 0.1080	5.280 0.0119 0.1080	5.490 0.0138 0.1080	5.540 0.0143 0.1090	5.870 0.0185 0.1090	6.020 0.0210 0.1090	6.150 0.0235 0.1090	6.300 0.0269 0.1100	6.410 0.0299 0.1100	6.510 0.0329 0.1100	6.600 0.0359 0.1100	6.690 0.0394 0.1100	6.770 0.0427 0.1100	6.880 0.0480 0.1110	6.960 0.0520 0.1110					
8.0-8.99				1.210 0.0035 0.0850	1.960 0.0044 0.0880	3.460 0.0052 0.0920	4.040 0.0062 0.0930	4.460 0.0074 0.0940	4.800 0.0088 0.0950	5.020 0.0100 0.0950	5.220 0.0114 0.0950	5.440 0.0133 0.0960	5.590 0.0148 0.0960	5.730 0.0165 0.0960	5.850 0.0182 0.0960	5.960 0.0199 0.0960	6.110 0.0227 0.0970	6.210 0.0248 0.0970	6.300 0.0269 0.0970	6.380 0.0290 0.0970	6.470 0.0316 0.0970	6.540 0.0339 0.0970	6.610 0.0363 0.0970	6.680 0.0390 0.0970	6.750 0.0419 0.0970	6.840 0.0460 0.0980
9.0-9.99					1.000 0.0029 0.0750	1.230 0.0036 0.0760	1.770 0.0043 0.0780	3.230 0.0050 0.0820	3.810 0.0058 0.0830	4.230 0.0067 0.0840	4.480 0.0075 0.0840	4.770 0.0087 0.0850	4.960 0.0097 0.0850	5.120 0.0107 0.0850	5.330 0.0123 0.0850	5.470 0.0136 0.0860	5.580 0.0147 0.0860	5.690 0.0160 0.0860	5.800 0.0175 0.0860	5.890 0.0188 0.0860	5.980 0.0202 0.0860	6.110 0.0227 0.0870	6.190 0.0244 0.0870	6.270 0.0261 0.0870	6.340 0.0280 0.0870	6.410 0.0299 0.0870
10.0-10.99							1.020 0.0030 0.0680	1.230 0.0036 0.0690	1.560 0.0041 0.0700	2.700 0.0047 0.0730	3.220 0.0050 0.0740	3.650 0.0055 0.0750	4.230 0.0067 0.0760	4.440 0.0074 0.0760	4.710 0.0084 0.0770	4.870 0.0092 0.0770	5.010 0.0100 0.0770	5.150 0.0109 0.0770	5.260 0.0117 0.0770	5.420 0.0132 0.0780	5.540 0.0143 0.0780	5.640 0.0154 .00780	5.730 0.0165 0.0780	5.810 0.0176 0.0780	5.880 0.0186 0.0780	5.960 0.0199 0.0780
11.0-11.99									1.010 0.0029 0.0620	1.180 0.0035 0.0630	1.450 0.0040 0.0640	1.920 0.0044 0.0650	2.930 0.0048 0.0670	3.500 0.0053 0.0680	3.910 0.0060 0.0690	4.130 0.0064 0.0690	4.380 0.0070 0.0700	4.580 0.0079 0.0700	4.730 0.0085 0.0700	4.870 0.0092 0.0700	4.970 0.0098 0.0700	5.110 0.0106 0.0700	5.230 0.0114 0.0700	5.360 0.0126 0.0700	5.480 0.0136 0.0710	5.540 0.0143 0.0710
12.0-12.99													1.260 0.0036 0.0580	1.540 0.0041 0.0590	2.050 0.0045 0.0600	3.020 0.0048 0.0620	3.450 0.0052 0.0630	3.760 0.0057 0.0630	4.000 0.0061 0.0640	4.270 0.0068 0.0640	4.420 0.0073 0.0640	4.550 0.0078 0.0640	4.650 0.0082 0.0640	4.810 0.0090 0.0650	4.950 0.0099 0.0650	5.090 0.0105 0.0650
13.0-13.99				First number: γ Second number: a Third number: f_p $\omega_p = 2\pi f_p$										1.040 0.0030 0.0530	1.140 0.0034 0.0540	1.320 0.0038 0.0540	1.680 0.0043 0.0550	2.150 0.0045 0.0560	2.830 0.0047 0.0570	3.360 0.0051 0.0580	3.710 0.0056 0.0580	3.920 0.0060 0.0590	4.100 0.0064 0.0590	4.250 0.0068 0.0590	4.300 0.0070 0.0590	4.440 0.0073 0.0580
14.0-14.99																		1.190 0.0035 0.0500	1.290 0.0037 0.0500	1.570 0.0042 0.0510	2.030 0.0045 0.0520	2.670 0.0047 0.0530	3.120 0.0048 0.0536	3.440 0.0052 0.0540	3.650 0.0055 0.0540	3.780 0.0067 0.0550
15.0-15.99																									2.900 0.0048 0.0500

Table 4. Parameters of the JONSWAP spectrum as function of H_s and T_z (Almar-Næss, 1985).

3.5 Structural dynamics

The need of dynamic analysis of structures is based on the fact that in many cases the loading that is applied to a structure varies with time, for example wave loading. When the loading varies with time the response of the structure will also vary according to the time series of the loading itself. A single degree of freedom system is the simplest model to describe this dynamics. Consider a system in Figure 13 which consists of mass m, spring stiffness k, and damping c.

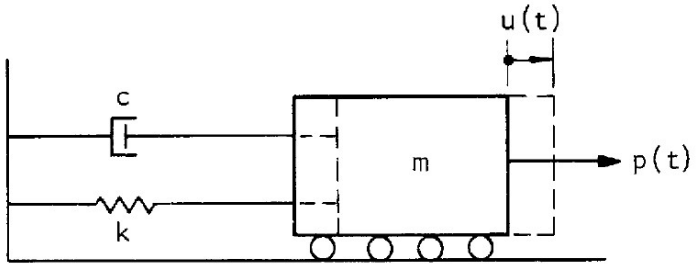

Figure 13. A mass-spring damper system (Chopra, 1980).

The spring stiffness k will create force $-ku$ (negative since the spring force direction is opposite the translation direction) while the mass m will produce force $m\ddot{u}$ according to Newton's second law of motion. The damper gives force $-c\dot{u}$. If there are no any external forces $(p=0)$ then the equation of motion of the system is:

$$m\ddot{u}+c\dot{u}+ku=0 \tag{3-34}$$

which is a homogeneous ordinary differential equation.

If the damping coefficient c is assumed to be zero (i.e. no damping), then equation (3-34) has general solution:

$$u(t)=u_0\sin\omega_n t+\frac{\dot{u}_0}{\omega_n}\cos\omega_n t \tag{3-35}$$

where

ω_n = natural frequency of the system = $\sqrt{\frac{k}{m}}$

u_0 = initial position of the mass

$\dot{u}_0$ = initial velocity of the mass

which u_0 and $\dot{u}_0$ are referred also as the initial conditions.

In reality damping will always exist in structural dynamics. This damping is often called also as viscous damping. As damping is difficult to be measured, two new variables will be introduced for this situation, they are the critical damping $c_{cr} = \sqrt{km}$ and the damping ratio $\zeta = c/c_{cr}$.

The vibrating system is considered as underdamped, critically damped, or overdamped when the damping ratio ζ is less than, equals to, or more than 1.0, respectively (see Figure 14 for reference). General solution for a system with damping is given below:

$$u(t) = e^{-\zeta\omega_n t}\left(u_0 \cos\omega_d t + \frac{\dot{u}_0 + u_0\zeta\omega_n}{\omega_d}\sin\omega_d t\right) \qquad (3\text{-}36)$$

where

ω_d = damped frequency of the system = $\omega_n\sqrt{1-\zeta^2}$

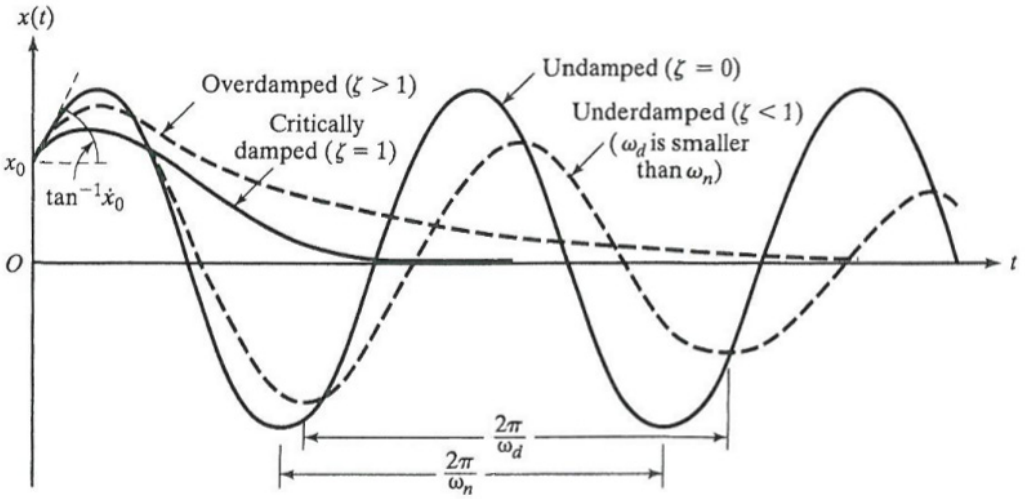

Figure 14. Illustration of different types of damping condition (Rao, 2004).

When the mass/structure is excited by external harmonic loading $p(t) = p_0 \sin\bar{\omega}t$ with $\bar{\omega}$ is the loading frequency, equation (3-33) should be rewritten as:

$$m\ddot{u} + c\dot{u} + ku = p_0 \sin\bar{\omega}t \qquad (3\text{-}37)$$

Equation (3-37) is a non-homogeneous differential equation hence it will have both homogeneous solution y_h and particular solution y_p and its general solution is $u(t) = y_h(t) + y_p(t)$. Derivation of solution gives the total response for this case:

$$u(t) = e^{-\zeta\omega_n t}\left(A\cos\omega_d t + B\sin\omega_d t\right) + \frac{p_0}{k}\frac{1}{\sqrt{\left(1-r^2\right)^2 + \left(2r\zeta\right)^2}}\sin\left(\overline{\omega}t - \theta\right) \qquad (3\text{-}38)$$

where

r = frequency ratio = $\dfrac{\overline{\omega}}{\omega_n}$

θ = phase lag between applied force and the response = $\tan^{-1}\left(\dfrac{2r\zeta}{\left(1-r^2\right)}\right)$

To be noticed that values of A and B in equation (3-38) depend on initial conditions that satisfy the whole of the equation. The homogeneous solution part of equation (3-38) will decay with time hence it is called as transient response and the particular solution part is called as steady-state response.

The p_0/k amplitude can be quickly understood as static response amplitude u_{st} of the mass due to force p_0 and spring stiffness k. When the transient response becomes so small and neglectable the ratio of total response and static response amplitude becomes:

$$\frac{u(t)}{u_{st}} = \frac{1}{\sqrt{\left(1-r^2\right)^2 + \left(2r\zeta\right)^2}} = DAF \qquad (3\text{-}39)$$

where

DAF = dynamic amplification factor

From equation (3-39) above it can be seen that DAF varies along with frequency ratio r and damping ratio ζ. When damping is small and loading frequency is close to the natural frequency, the system will experience high magnification of response amplitude (see Figure 15).

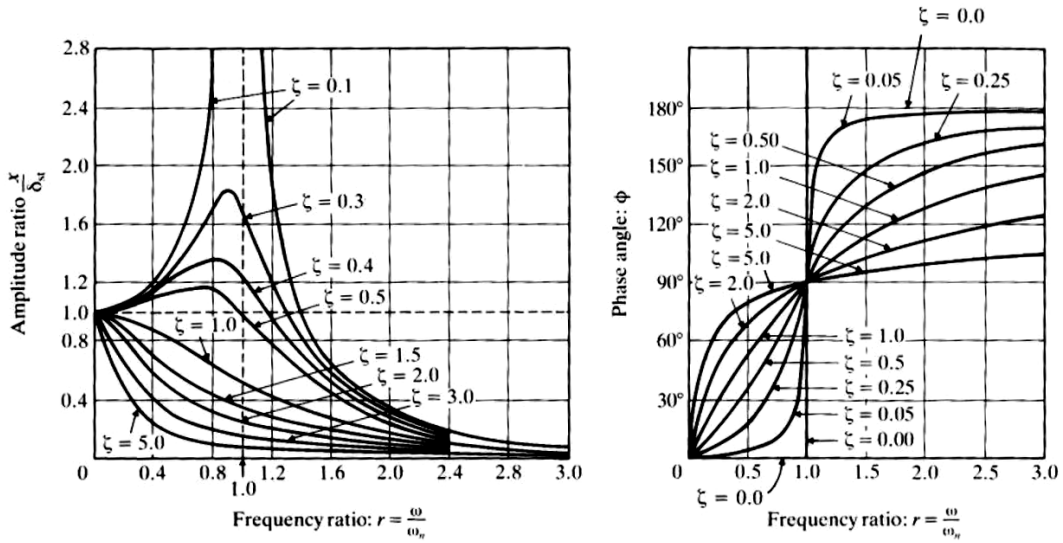

Figure 15. DAF and θ as function of frequency ratio r (Rao, 2004).

3.6 Pipe circumferential stress due to pressure

The stress resulted from hydrostatic pressure (external and internal pressure) acting on hollow pipe is called circumferential/hoop stress. The fundamental of this stress can be derived by examining the following illustration (Figure 16).

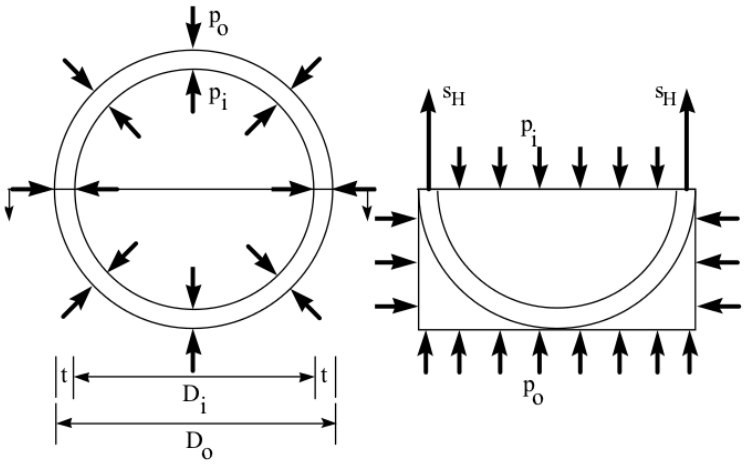

Figure 16. Circumferential stress in a pipe (Palmer and King, 2004).

Since the summation of forces in horizontal direction should be zero due to symmetry, pressure component in the left and right side of pipe will eliminate each other. In vertical direction the summation of forces (per unit length) can then be written as:

$$p_o D_o + 2S_H t - p_i D_i = 0 \tag{3-40}$$

$$S_H = \frac{p_i D_i - p_o D_o}{2t} \tag{3-41}$$

where

S_H = circumferential/hoop stress

p_i = internal pressure

p_o = external pressure

D_i = internal diameter of pipe

D_o = external diameter of pipe

t = wall thickness

Various methods for calculating circumferential stress above exist and the simplest and also commonly used is the Barlow formula:

$$S_H = \frac{p_i D_o}{2t} \tag{3-42}$$

Quick look at both equation (3-41) and (3-42) gives common conclusion that the latter is more conservative as it neglects the external pressure term $p_o D_o$. The Barlow formula overestimates the maximum hoop stress, but nevertheless many code commitees specify to use it (Palmer and King, 2004).

Chapter 4
Design Criteria

Several major institutions publish their own codes/regulations about design criteria for marine drilling riser system and each of these codes can be more conservative than the other and vice versa.

Det Norske Veritas (DNV) publishes one international standard suitable for design and analysis of top tensioned riser systems operated from floaters in DNV-OS-F201 Dynamic Risers. This standard is applicable for pipes having outer diameter to wall thickness ratio D/t less than 45 (DNV, 2010). Steel drilling risers are included in the scope of this standard. Working Stress Design (WSD) method, a long-established conservative method which is simple to understand, is available and may be used to obtain the acceptance criteria according to the standard.

American Petroleum Institute (API) also has its own standard which is published in API RP 16Q Design, Selection, Operation, and Maintenance of Marine Drilling Riser Systems.

Another one is EN ISO 13624-1 Part 1: Design and operation of marine drilling riser equipment. In the API and ISO standard there are three different criterias for three different modes which are drilling, non-drilling, and riser disconnected criteria. Some brief explanations about the standard from each committee will be described in the next several subchapters and refer to each respective standards.

4.1 DNV-OS-F201 criteria

Steel pipe/riser members shall be designed to withstand both internal and external overpressure, if any. Internal overpressure leads to bursting failure and external overpressure leads to hoop buckling (collapse) and also propagating buckling failure.

Bursting criteria:

$$\left(p_{li} - p_e\right) \leq \frac{p_b(t_1)}{\gamma_m \gamma_{SC}}$$

with

$$p_b(t_1) = \frac{2}{\sqrt{3}} \frac{2t}{D - t_1} min\left(f_y; \frac{f_u}{1.15}\right)$$

is the burst resistance. The minimum required wall thickness without including any tolerances and allowances (due to fabrication and corrosion) is then given immediately by:

$$t_1 = \frac{D}{\frac{4}{\sqrt{3}} \frac{min\left(f_y; \frac{f_u}{1.15}\right)}{\gamma_m \gamma_{SC}\left(p_{li} - p_e\right)} + 1}$$

where

p_{li} = local incidental pressure $= \left(p_d + \rho_i g h\right) + 0.1 p_d$

p_e = external pressure

γ_m = material resistance factor

γ_{SC} = safety class resistance factor

p_d = maximum surface design pressure during normal operations

ρ_i = internal fluid density

h = internal fluid column height

g = acceleration of gravity

f_y = yield stress = $\left(SMYS - f_{y,temp}\right)\alpha_U$

f_u = tensile strength = $\left(SMTS - f_{u,temp}\right)\alpha_U$

D = pipe outer diameter

t_1 = pipe wall thickness excluding fabrication and corrosion tolerances

$SMYS$ = specific minimum yield stress

$f_{y,temp}$ = temperature derating factor for the yield stress

$SMTS$ = specific minimum tensile strength

$f_{u,temp}$ = temperature derating factor for the tensile strength

α_U = material strength factor, to be taken as 0.96 for normal condition, or 1.0 if supplementary requirement ensuring increased confidence in material strength is fulfilled

Values for γ_m and γ_{SC} which are material and safety class resistance factor, respectively, are given in Table 5. Abbreviations of ULS, ALS, SLS, and FLS are Ultimate, Accidental, Serviceability, and Fatigue Limit State, respectively.

Material resistance factor γ_m		**Safety class resistance factor γ_{SC}**		
ULS & ALS	**SLS & FLS**	**Low**	**Normal**	**High**
1.15	1.0	1.04	1.14	1.26

Table 5. Material and safety class resistance factors (DNV, 2010).

Hoop buckling (collapse) criteria:

$$(p_e - p_{min}) \leq \frac{p_c(t_1)}{\gamma_m \gamma_{SC}}$$

where

p_{min} = minimum internal pressure

p_c = hoop buckling resistance, given by solving the following equation:

$$(p_c(t) - p_{el}(t))\left(p_c^{\,2}(t) - p_p^{\,2}(t)\right) = p_c(t)\,p_{el}(t)\,p_p(t)\,f_0\,\frac{D}{t}$$

The solution for variable p_c above can be found derived in the commentary section of DNV-OS-F101 Submarine Pipeline Systems as follow:

$$p_{el}(t) = \frac{2E\left(\frac{t}{D}\right)^3}{1-v^2}$$

$$p_p(t) = f_y \alpha_{fab} \frac{2t}{D}$$

$$p_c = y - \frac{1}{3}b$$

with supporting formulas as follow:

$$b = -p_{el}(t)$$

$$c = -\left(p_p(t)^2 + p_p(t)p_{el}(t)f_0\frac{D}{t}\right)$$

$$d = p_p(t)^2 p_{el}(t)$$

$$u = \frac{1}{3}\left(-\frac{1}{3}b^2 + c\right)$$

$$v = \frac{1}{2}\left(\frac{2}{27}b^3 - \frac{1}{3}bc + d\right)$$

$$\Phi = \cos^{-1}\left(\frac{-v}{\sqrt{-u^3}}\right)$$

$$y = -2\sqrt{-u}\cos\left(\frac{\Phi}{3} + \frac{60\pi}{180}\right)$$

Propagating buckling criteria:

$$(p_e - p_{min}) \leq \frac{p_{pr}}{\gamma_m \gamma_{SC} \gamma_c}$$

where

p_{pr} = buckling propagation resistance = $35 f_y \alpha_{fab}\left(\frac{t_2}{D}\right)^{2.5}$

t_2 = pipe wall thickness excluding corrosion tolerances only

α_{fab} = fabrication factor, to be taken as 1.0 for seamless pipe

γ_c = condition factor, to be taken as 1.0 if no buckle propagation is allowed after buckling was initiated, or 0.9 if it is allowed for a short distance.

Working stress design criteria:

Working Stress Design criteria for combined loading according to DNV may be used for pipes with D/t ratio less than 30. The previous load effect factors and resistance factors are not to be used here and substituted by unity instead. The criteria is divided into two formulations, for pipe members subjected to net internal overpressure:

$$\left\{\left(\frac{|M|}{M_k}\sqrt{1-\left(\frac{p_{ld}-p_e}{p_b(t_2)}\right)^2}\right)+\left(\frac{T_e}{T_k}\right)^2\right\}+\left(\frac{p_{ld}-p_e}{p_b(t_2)}\right)^2 \le \eta^2$$

and for pipe members subjected to net external overpressure it shall satisfy:

$$\left\{\frac{|M|}{M_k}+\left(\frac{T_e}{T_k}\right)^2\right\}^2+\left(\frac{p_e-p_{min}}{p_c(t_2)}\right)^2 \le \eta^4$$

where

M = bending moment

M_k = plastic bending moment resistance = $f_y\alpha_c(D-t_2)^2 t_2$

p_{ld} = local internal design pressure = $p_d+\rho_i gh$

T_e = effective tension

T_k = plastic axial force resistance = $f_y\alpha_c\pi(D-t_2)t_2$

η = usage factor for combined loading

α_c = parameter accounting for strain hardening and wall thinning, given by:

$$\alpha_c=(1-\beta)+\beta\frac{f_u}{f_y}$$

$$\beta=\begin{cases}(0.4+q_h) & \text{for } \dfrac{D}{t_2}<15\\ \dfrac{(0.4+q_h)}{45}\left(60-\dfrac{D}{t_2}\right) & \text{for } 15<\dfrac{D}{t_2}<60\\ 0 & \text{for } 60<\dfrac{D}{t_2}\end{cases}$$

$$q_h=\begin{cases}\dfrac{(p_{ld}-p_e)}{p_b(t_2)}\dfrac{2}{\sqrt{3}} & \text{for } p_{ld}>p_e\\ 0 & \text{else}\end{cases}$$

Guidance note from DNV for the net internal overpressure criteria above is that the criteria may be regarded as plastic Von Mises criterion and is equivalent to the plastic limit bending capacity including the effect of strain hardening and wall thinning for $T_e / T_k \ll 1$. It will reduce to the traditional wall thickness Von Mises criteria for case of pressure and effective tension load effects only.

The usage factor η for this working stress design criteria and the descriptions for the corresponding safety classes can be seen in the following Table 6 and Table 7.

Low	Normal	High
0.83	0.79	0.75

Table 6. Usage factor η for different safety classes (DNV, 2010).

Safety Class	Definition
Low	Where failure implies low risk of human injury and minor environmental and economic consequences.
Normal	For conditions where failure implies risk of human injury, significant environmental pollution or very high economic or political consequences.
High	For operating conditions where failure implies high risk of human injury, significant environmental pollution or very high economic or political consequences.

Table 7. Classification of safety classes (DNV, 2010).

4.2 API RP 16Q criteria

For plain round pipe, API uses the von Mises yield criterion for combination of three principal stresses at each pipe section which are radial, hoop and axial stresses. Design and operating limits for the key riser parameters such as upper and lower flex/ball joint angles, allowable stresses, and tension settings are to be maintained during the operation. Table 8 provides the recommended design criteria for three different operating modes of drilling riser.

Design Parameter	Riser Connected		Riser Disconnected
	Drilling	Non-Drilling	
Mean flex/ball joint angle (upper & lower)	2^o	N/A	N/A
Max flex/ball joint angle (upper & lower)	4^o	90% available	90% available
Stress criteria: 1. Method "A" - Allowable stress 2. Method "B" - Allowable stress - Significant dynamic stress range: @ SAF ≤ 1.5 @ SAF > 1.5	 0.4 σ_y 0.67 σ_y 10 ksi 15÷SAF	 0.67 σ_y 0.67 σ_y N/A N/A	 0.67 σ_y 0.67 σ_y N/A N/A
Minimum top tension	T_{min}	T_{min}	N/A
Dynamic tension limit	DTL	DTL	N/A
Max tension setting	90% DTL	90% DTL	N/A

Table 8. Drilling risers operating and design guidelines (API, 1993).

Method "A" is suitable for most water depth areas while method "B" is more recommended for deepwater areas. The criteria on significant dynamic stress range limitation has a purpose to provide some control on fatigue damage accumulated by the riser. The dynamic tension limit (DTL) is tensioner rating which is defined by the manufacturer. Maximum tension is obtained including dynamic variations and shall not exceed the required setting above.

The von Mises stress criterion is calculated as:

$$\frac{1}{\sqrt{2}}\sqrt{\left(\sigma_{pr}-\sigma_{p\theta}\right)^2+\left(\sigma_{p\theta}-\sigma_{pz}\right)^2+\left(\sigma_{pz}-\sigma_{pr}\right)^2}$$

where

σ_{pr} = radial stress

$\sigma_{p\theta}$ = hoop stress

σ_{pz} = axial including bending stress

σ_y = minimum yield strength of material

The riser should be designed to always have positive effective tension in all parts of its body. Minimum top tension T_{min} is determined using following criteria:

$$T_{min} = \frac{T_{SRmin} N}{R_f (N - n)}$$

with

$$T_{SRmin} = W_s f_{wt} - B_n f_{bt} + A_i (d_m H_m - d_w H_w)$$

where

T_{SRmin} = minimum slip ring tension

N = number of tensioners supporting the riser

R_f = reduction factor to account for fleet angle and mechanical efficiency, to be taken as 0.95 for drilling and 0.9 for non-drilling

n = number of tensioners subject to sudden failure (at least one)

W_s = submerged weight of bare riser

f_{wt} = submerged weight tolerance factor, minimum is 1.05 unless accurately weighed

B_n = net positive buoyancy (lift force)

f_{bt} = buoyancy loss and tolerance factor, maximum is 0.96 unless accurately measured

A_i = internal cross sectional area of riser, including all lines

d_m = drilling fluid density

H_m = drilling fluid column height

d_w = sea water density

H_w = sea water column height

4.3 ISO 13624-1 criteria

ISO 13624-1:2009 criteria is relatively almost similar to the API RP 16Q. There are some differences for criteria on flex/ball joint angles upper bounds. Table 9 gives the guidelines for recommended design practices for different modes of drilling riser:

Design Parameter	Riser Connected		Riser Disconnected
	Drilling	Non-Drilling	
Mean upper flex/ball joint angle	1^o to 1.5^o	N/A	N/A
Max. upper flex/ball joint angle	5^o	90% available (or contact with moonpool structure)	90% available (or contact with moonpool structure)
Mean lower flex joint angle	2^o	N/A	N/A
Max. lower flex joint angle	5^o	90% available	90% available
Stress criteria: 1. Method "A" - Allowable stress 2. Method "B" - Allowable stress - Significant dynamic stress range: @ SAF ≤ 1.5 @ SAF > 1.5	 $0.4\ \sigma_y$ $0.67\ \sigma_y$ 10 ksi 15÷SAF	 $0.67\ \sigma_y$ $0.67\ \sigma_y$ N/A N/A	 $0.67\ \sigma_y$ $0.67\ \sigma_y$ N/A N/A
Minimum top tension	T_{min}	T_{min}	N/A
Dynamic tension limit	DTL	DTL	N/A
Max tension setting	90% DTL	90% DTL	N/A

Table 9. Drilling risers maximum design guidelines (ISO, 2009).

Same von Mises criteria as from API to be used here. Calculation of T_{min} uses same formulation from API as well. The mean and maximum flex/ball joint angles are to be maintained as small as possible to prevent damage to the riser, flex/ball joints (because of rating from the manufacturer) and the LMRP/BOP stack.

The upper flex/ball joint angle should also consider clearance in the moonpool area. ISO standard also mentions that the top tension to be maintained at a safe level above the API minimum tension T_{min} in normal operations to accommodate the dynamic tension variations that may cause the riser tension to fall below the minimum value required.

Chapter 5
Orcaflex Software

Orcaflex is one of many 3-dimensional finite element programs commercially available for offshore pipeline/riser structural analysis. This chapter will describe the principle that is behind the Orcaflex software which is used for the analysis in this work. Descriptions in this chapter are referring to Orcaflex Manual version 9.5a (Orcina, 2011).

First of all it should be understood the 3-dimensional coordinate systems convention in Orcaflex which are defined in Figure 17.

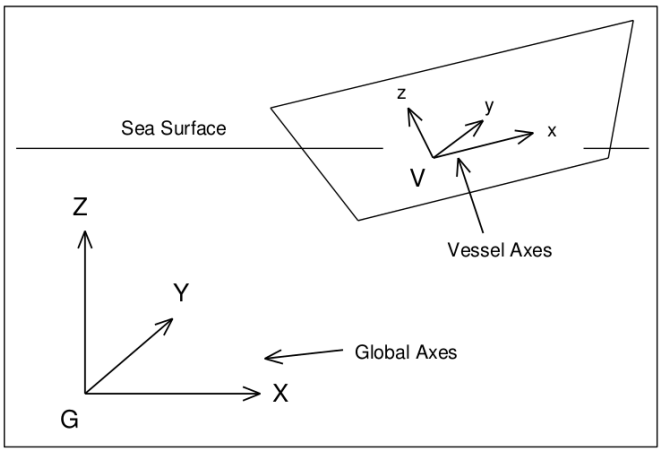

Figure 17. Coordinate systems (Orcina, 2011).

Coordinate systems in Orcaflex can be separated as global axes GXYZ with direction GX, GY, and GZ and also local axes Lxyz. For example, in Figure 17 above the vessel has its own local axes Vxyz with direction Vx, Vy, and Vz.

The conventions for directions and headings in Orcaflex are measured relative to axes where they are located on as presented in Figure 18. Waves, current, and wind directions are specified as the directions where they are progressing to, and relative to global axes. Vessel headings are also relative to global axes and

defined as the direction where its *Vx*-axis is pointing to. When *Vx*-axis is pointing to *x* direction in Figure 18, a 180^{o} wave means a wave coming from bow towards stern of the vessel.

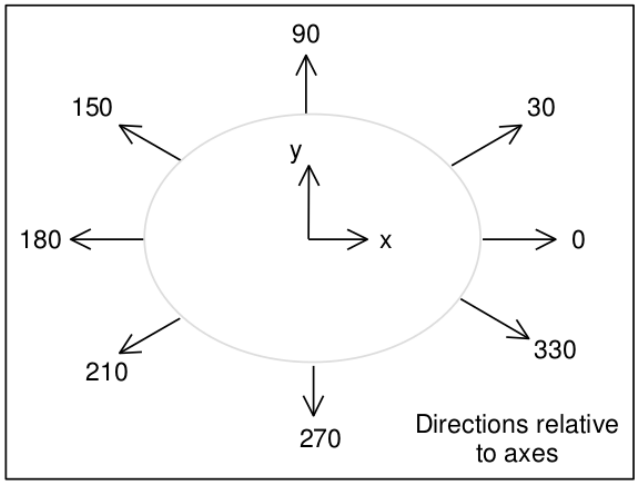

Figure 18. Directions and headings conventions (Orcina, 2011).

Orcaflex models lines as discrete elements as shown in Figure 19. The elements consist of nodes and segments. Segments will keep only the axial and torsional properties while nodes will keep the other properties such as mass, weight, and buoyancy which are equally divided into two for each segments.

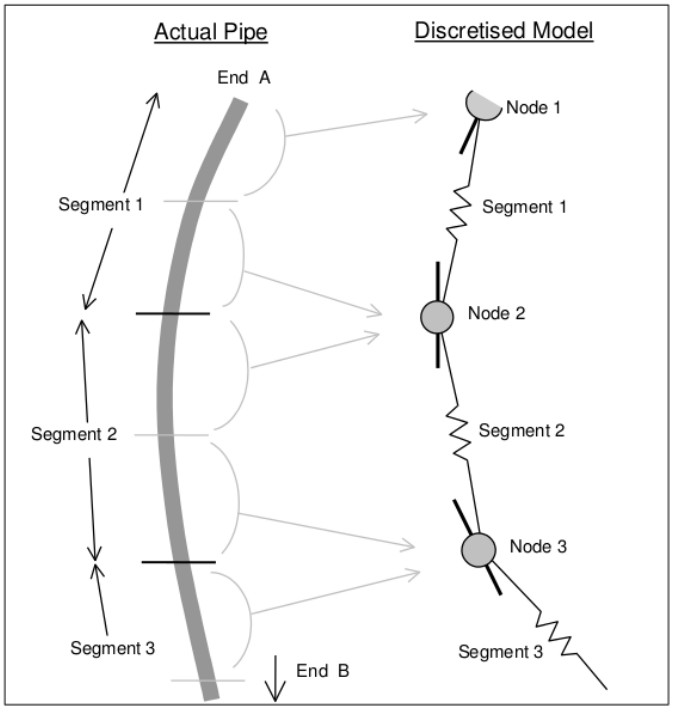

Figure 19. Discretized line model (Orcina, 2011).

Static analysis in Orcaflex has two main objectives; to find equilibrium position of the lines under mass, weight, buoyancy, and current drag force and to provide starting profile for dynamic analysis/simulation. Dynamic analysis executes time simulation of the motions of the system/model over a specified period of time. Simulation time origin can be adjusted to a specific time of interest. This is useful for quick look on how the system behaves during a particular time. A facility called View Profile for a desired wave train is available to give an overview of the time series of an irregular wave for that purpose.

The equation of motion in Orcaflex is given as:

$$M(p,a)+C(p,v)+K(p)=F(p,v,t)$$

where

$M(p,a)$ = system inertia load function

$C(p,v)$ = system damping load function

$K(p)$ = system stiffness load function

$F(p,v,t)$ = external load function

p,v,a,t = position, velocity, and acceleration vector, and time, respectively.

Two schemes are available in Orcaflex for solving the equation of motion; explicit and implicit integration. In explicit integration scheme, the equation of motion is solved using forward Euler method with constant time step. From static configuration (which is obtained from static analysis) all forces and moments, including hydrodynamic loads, which are acting on each node are calculated and local equation of motion for each node is then computed numerically. The equation is solved at the beginning of the time step. The other scheme, implicit integration scheme, uses the "generalised-α" integration method to solve the equation after applying all forces and moments using same procedure as explained before. This implicit integration method solves the equation of motion at the end of the time step.

For calculation of hydrodynamic load on lines, Orcaflex uses an extended form of Morison's equation (see also Subchapter 3.3 for reference) integrated over a body as follow:

$$F_w = \left(\Delta a_w + C_a \Delta a_r\right) + \frac{1}{2}\rho C_D A V_r |V_r|$$

where

F_w = fluid force

Δ = mass of fluid displaced by the body

a_w = fluid acceleration relative to earth

C_a = added mass coefficent for the body

a_r = fluid acceleration relative to the body

ρ = density of water

C_D = drag coefficient for the body

A = projected drag area (product of drag diameter and segment length)

V_r = fluid velocity relative to the body.

Fluid velocity is separated into its normal and parallel components to the line local axis for computation of drag force. This is called as cross flow principle in Orcaflex. This is used for convention purpose since using resultant fluid velocity to get the resultant drag force and then divide it into normal and parallel drag components will not give the same result due to nonlinearity of drag term.

Principal stresses for von Mises combined stress criterion are obtained from three eigenvalues of Orcaflex stress component matrix. The matrix is given by:

$$\begin{pmatrix} \sigma_{RR} & \sigma_{RC} & \sigma_{RZ} \\ \sigma_{RC} & \sigma_{CC} & \sigma_{CZ} \\ \sigma_{RZ} & \sigma_{CZ} & \sigma_{ZZ} \end{pmatrix}$$

and with reference from theory of mechanics of solids (Boresi, et al., 2003) they are calculated using Lamé's equation for thick-walled cylinder as:

σ_{RR} = radial stress $= A - \frac{B}{r^2} = \frac{p_1 a^2 - p_2 b^2}{b^2 - a^2} - \frac{a^2 b^2 (p_1 - p_2)}{(b^2 - a^2) r^2}$

σ_{CC} = hoop stress $= A + \frac{B}{r^2} = \frac{p_1 a^2 - p_2 b^2}{b^2 - a^2} + \frac{a^2 b^2 (p_1 - p_2)}{(b^2 - a^2) r^2}$

σ_{ZZ} = axial stress $= \sigma_t + \sigma_b$

where (see Figure 20 for reference)

r, θ = point location in angular coordinate

p_1, p_2 = internal and external pressure, respectively

a, b = inner and outer pipe radius, respectively

σ_t = direct tensile stress $= \frac{T_w}{A_z}$

σ_b = bending stress $= \frac{r(M_x \sin\theta - M_y \cos\theta)}{I_{xy}}$

T_w = wall tension

A_z = cross section area

M_x, M_y = bending moment components about x and y axis, respectively

I_{xy} = moment of inertia about x or y axis

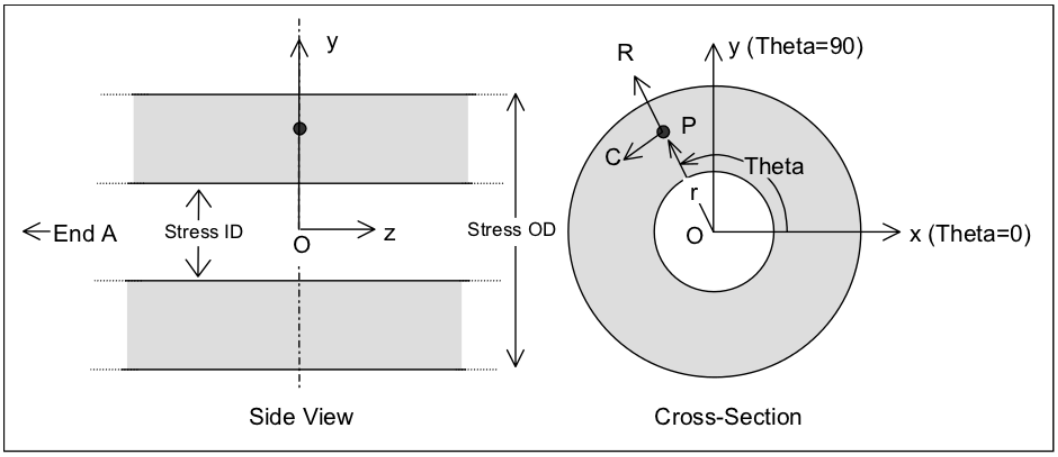

Figure 20. Reference for stress calculation (Orcina, 2011).

The remaining shear stresses from the stress component matrix are given using equation below:

$$\sigma_{RC} = 0$$

$$\sigma_{RZ} = \frac{S_x \cos\theta - S_y \sin\theta}{A_z}$$

$$\sigma_{CZ} = \frac{S_x \cos\theta - S_y \sin\theta}{A_z} + \sigma_\tau$$

where

S_x, S_y = shear force components in *xy* plane

σ_τ = shear stress due to torque $= \frac{\tau r}{I_z}$

τ = torsion

I_z = moment of inertia about *z* axis $= 2I_{xy}$

The effective and wall tension (see also Subchapter 3.2) are related in Orcaflex using the following formula:

$$T_e = T_w + \left(P_o A_o - P_i A_i\right)$$

$$T_w = EA\varepsilon - 2v\left(P_o A_o - P_i A_i\right) + EAe\left(\frac{dL/dt}{L_0}\right)$$

where

T_e, T_w = effective and wall tension, respectively

ε = total mean axial strain $= \frac{\left(L - \lambda L_0\right)}{\lambda L_0}$

L = instantaneous length of segment

L_0 = unstretched length of segment

v = Poisson ratio

P_i, P_o = internal and external pressure, respectively

A_i, A_o = internal and external cross sectional stress area, respectively

e = damping coefficient of the line, in seconds

dL/dt = rate of increase of length

Both effective and wall tension are relevant for measurement of pipe buckling due to pressure. Further reference regarding this can be obtained from a paper by Palmer and Baldry (1974). Figure 21 illustrates the schematic diagram for effective and wall tension in Orcaflex.

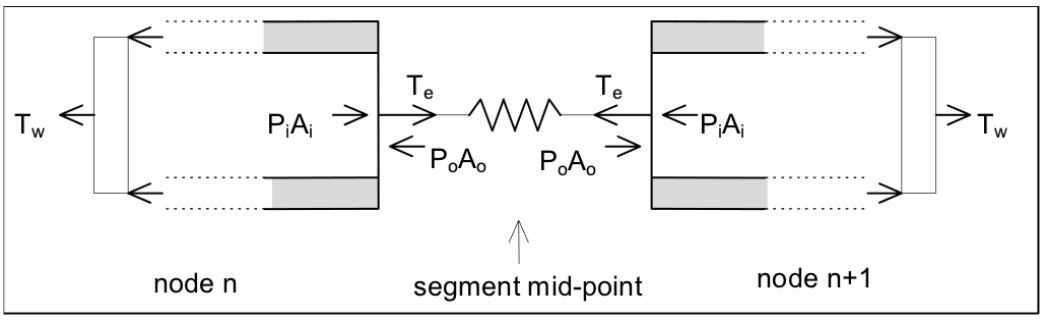

Figure 21. Reference for tension and pressure forces (Orcina, 2011).

Chapter 6
Analysis Methodology

The drilling riser analysis in this work will be conducted in two separate stages. The first stage is to determine the required profiles/characteristics for drilling at 10000 ft (around 3000 m) water depth using conventional 21 inch riser by taking into account the tensioner capacity and capability of the drilling rig used in the analysis to illustrate the ultra-deepwater drilling depth achievement so far (see Subchapter 1.1). The second stage will be to analyze a similar case of drilling operation only now using slim 16 inch riser instead and find out how it will work for even deeper water area. Configuration for both 21 inch and 16 inch riser for analysis will be described in the next subchapters.

6.1 Configuration for 21 inch drilling riser

Water depth to be used for application of this 21 inch riser is selected as 3018 m. A sixth generation rig of Odfjell Drilling, the Deepsea Stavanger, which is rated for operation at 3000 m water depth region (Odfjell Drilling, 2012) will be utilized for analysis. Connection point of upper flex/ball joint on the rig is at approximately 27.5 meter above the sea surface. The rig properties e.g. tensioner properties, slip joint outer and inner barrel properties, and rig motion characteristics are obtained from data from the company.

New riser joints and buoyancy module properties will be designed to satisfy the requirements for this specific ultra-deepwater drilling operation. Required tensioner forces (stiffnesses) and dampings will be interpolated linearly from the existing tensioner table whenever needed for simplicity. The maximum top tension available on the rig through its tensioners is 1450 ton (3200 kips) at full stroke 15 m with total number of tensioners onboard are 6 tensioners (Odfjell Drilling, 2012).

The expected result to be obtained in this 21 inch riser analysis is the safe riser configuration for operation in the desired water depth which should be within the stress and flex/ball joint angle limitations (as well as other criteria) as described in Chapter 4 and also the required riser top tension should not exceed the capacity of the rig's tensioner system. The heaviest drilling fluid to be used will be a 17 ppg drilling mud (specific gravity of 2.0). Since this heavy density fluid will give an enormous internal overpressure in ultra-deepwater then the new riser will be subject to burst failure check (see Subchapter 4.1 for reference on this).

The proposed configuration of the riser joints to be connected to the bottom of slip joint is illustrated in Figure 22. The assembly consists of 131 riser joints with length of 75 ft each. First couple of joints and the last joint of the riser are without any buoyancy module attached (bare riser). The main purpose of this is to reduce the effect of current drag force which is maximum near the sea surface (because of the current velocity profile that will be given later) but on the other hand it will make the riser heavier if less buoyancy module joints are used. An on-site installation practicality issue is also considered for justification of using bare riser joint at the end of assembly.

The length of the slip joint can be adjusted to fit the overall length of the drilling riser measured geometrically from the upper flex joint connection to the seabed. The upper end of riser joints assembly is connected to bottom end of outer barrel and lower end of the assembly is connected to Lower Marine Riser Package (LMRP) stack at elevation of approximately 15 m above seabed (this is roughly assumed to represent the total height of LMRP including BOP and wellhead height measured from the seabed).

The upper flex/ball joint was constructed by its manufacturer having a nonlinear rotational stiffness that will allow some rotations of the connected riser and hence will reduce the riser top end bending moment compared to a fixed end connection. Same situation applies for the lower flex/ball joint which is rated for 10000 ft

water depth for this case. The detailed nonlinear stiffness data are obtained from Odfjell Drilling and will be used as input for Orcaflex.

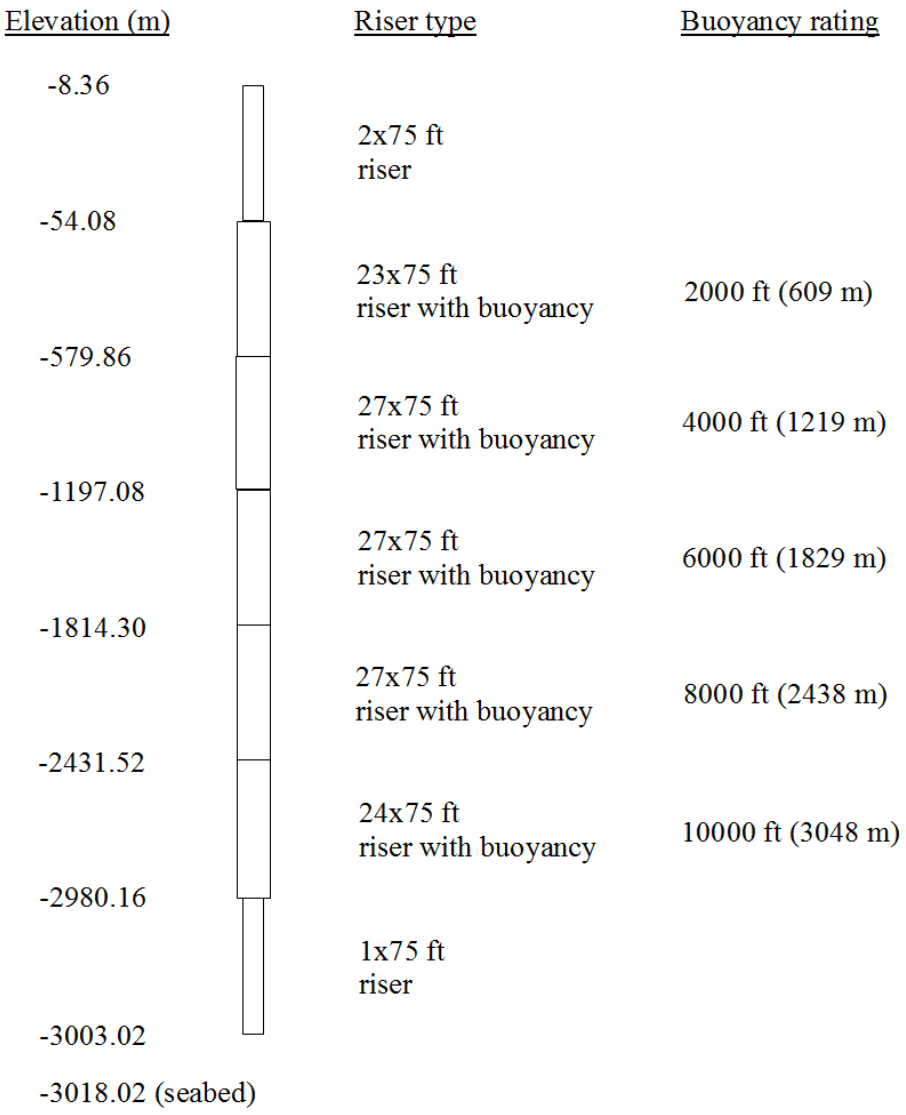

Figure 22. Proposed configuration for 21 inch drilling riser joints.

All risers to be used have wall thickness of 22.2 mm (0.875 in). The grade of the riser is API 5L X80 which has minimum yield stress 555 MPa (80.5 ksi) and minimum tensile strength obtained from API standard for grade X80 pipe is 625 MPa (90.6 ksi) (based on API Specification 5L, 2007). Several important properties of the riser joints and buoyancy modules can be seen in the following Table 10 to 12.

Riser Type	Outer Diameter (in)	Inner Diameter (in)	Length/ Joint (m)	Dry Weight (ton)
75 ft bare	21	19.25	22.86	12.93
75 ft + buoyancy (2000 ft)	56	19.25	22.86	23.95
75 ft + buoyancy (4000 ft)	56	19.25	22.86	24.95
75 ft + buoyancy (6000 ft)	56	19.25	22.86	26.45
75 ft + buoyancy (8000 ft)	56	19.25	22.86	28.21
75 ft + buoyancy (10000 ft)	56	19.25	22.86	29.44

Table 10. Main riser joint properties for 21 inch riser.

Buoyancy Type	Outer Diameter (in)	Inner Diameter (in)	Service Depth (m)	Net Buoyancy/ Joint (ton)	Material Density (kg/m^3)
Rating 2000 ft	56	21	609	14.75	353
Rating 4000 ft	56	21	1219	13.75	385
Rating 6000 ft	56	21	1829	12.26	433
Rating 8000 ft	56	21	2438	10.49	489
Rating 10000 ft	56	21	3048	9.26	529

Table 11. Buoyancy module properties for 21 inch riser.

Auxiliary Line Type	Outer Diameter (in)	Wall Thickness (in)	No. of Lines
Choke & kill line	6.5	1.0	2 (1 each)
Hydraulic line	2.88	0.28	2
Booster line	5	0.5	1

Table 12. Auxiliary line properties for 21 inch riser (Odfjell Drilling, 2012).

The wall thickness for the new 21 inch riser are selected based on DNV burst check requirement using 17 ppg of drilling mud inside the riser and the need to accommodate the combined stress criteria (mainly from hoop and tensile stress) to be below the limit. All riser joints (including bare risers) have auxiliary lines such as choke & kill lines, booster line, and hydraulic lines attached which will contribute weights to the main riser for conservative purpose.

The weights in Table 10 above are already including all those auxiliary lines in Table 12. A 10% of weight contingency was added to the calculation of weights to accommodate any uncertainties of riser joint weight which was not going through accurate measurement.

Buoyancy properties in Table 11 are derived based on buoyancy density properties obtained from the website of one manufacturer which is specialized in syntactic foam floatation for offshore drilling operations up to 12000 ft/3658 m (Cuming Corporation, 2012). Any required assumptions are made to give the most conservative condition for the calculation of these properties due to lack of real data from measurements or laboratory testing, such as loss of buoyancy, water absorption, and so on. For this reason, a 15% of buoyancy loss was applied to all calculations of buoyancy modules to acquire worse capacity of the buoyancy modules. Detailed calculations for all riser and buoyancy module properties including the auxiliary lines can be found in Appendix C.

An equivalent line for each riser joints will be created for modelling purpose in Orcaflex. This equivalent line will represent the assembly of main riser and its auxiliary lines (and buoyancy module in case of riser with buoyancy) so that it has the same properties as the original line including the weights and strengths. Drag diameter and stress diameter of the equivalent line need to be specified individually as well.

For risers with buoyancy, the drag diameter will be taken clearly as the outer diameter of the buoyancy module while for bare risers the drag diameter ideally should be obtained from full scale hydrodynamic analysis but in this case it will be taken as the summation of main riser diameter and choke & kill line diameter (see Figure 23) or $D + 2\mathrm{d}$ as per guideline from DNV Wellhead Fatigue Analysis Report (2011).

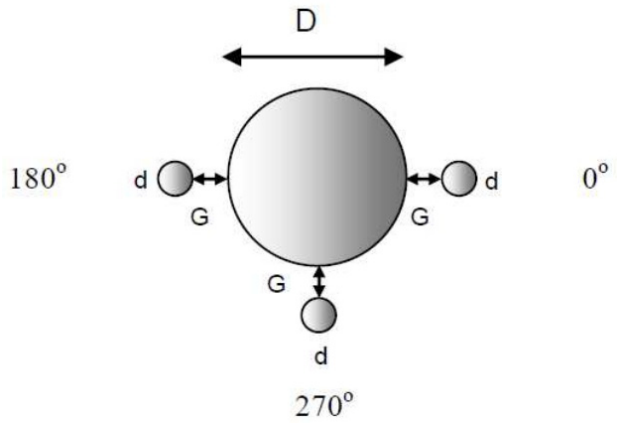

Figure 23. Illustration for equivalent drag diameter selection (DNV, 2011).

The guideline also gives the corresponding drag and added mass coefficient to be used if detailed data is not available. For this 21 inch riser the hydrodynamic coefficients will then be taken as recommended by the guideline which is 1.0 as the drag coefficient and 1.1 as the added mass coefficient when the suggested method for determination of drag diameter is employed (DNV, 2011).

6.2 Configuration for 16 inch drilling riser

The required top tension obtained from the 21 inch drilling riser analysis will be used as limitation for comparison with the required top tension for 16 inch riser. Since the weight of the 16 inch riser will be obviously lighter than the 21 inch one, then the required top tension can be immediately predicted to be less. For this reason the water depth for analysis will then be increased by keeping in mind that the resulted stress and angles will always be checked according to the limiting criteria as described in Chapter 4.

Same drilling rig will be used for analysis. Tensioner stiffnesses and damping properties will still use the same properties as the one from the 21 inch riser case. The heaviest drilling fluid density to be used for the analysis is same as in the previous 21 inch riser configuration to simulate a similar condition for comparison when executing drilling operation i.e. 17 ppg. Burst failure check will also be conducted here.

One assumption to be made is that the connection point at top riser end will just fit to the connection point at bottom of slip joint outer barrel. In reality, a tapered short section adaptor with special properties need to be installed in between the interface since the rig's slip joints are dedicated for operation using 21 inch conventional riser. Nevertheless, it is more conservative to use this assumption since the 16 inch riser properties are considered to be weaker.

The lower end of the riser is also connected to Lower Marine Riser Package (LMRP) stack at elevation of 15 m above seabed same as the case with 21 inch riser previously which represents the assumed total height of LMRP including BOP and wellhead heights measured from the seabed.

Wall thickness for the new slim 16 inch riser was selected through several iterations in order to obtain an optimum result with respect to required top tension and maximum combined stress when it is used for deepwater application with more than 10000 ft of desired target water depth. Wall thickness selection was based on DNV burst check requirement using 17 ppg of drilling mud, same as for the 21 inch riser. However, the combined stress (Von Mises) criteria was also required to be satisfied by the riser so a thicker wall thickness was always used during the iterations using different preliminary riser configurations. The resulted maximum combined stress was aimed to be as close as possible to the one resulted from the 21 inch riser case. Hoop stress, as well as tensile stress, was the main contributor for this. Progressive depth adjustments were conducted and the 16 inch riser profile was rebuilt and reanalyzed in every adjustment. The adjustment arrived at 3407.1 m depth using 19.05 mm (0.75 in) wall thickness.

The same drilling rig Deepsea Stavanger, will still be considered to be just capable to operate at this deeper water depth and will be used as it is without any changes for simplicity in this project.

The proposed configuration for the 16 inch riser joints to be analyzed is illustrated in Figure 24. The riser joints are newly designed for this particular case and

consists of 148 joints with length of 75 ft each. The upper flex/ball joint for this 16 inch riser case will use the same properties (nonlinear rotational stiffness) as the previous 21 inch riser case. However, to be noticed since the water depth goes beyond 11000 ft (3353 m) here, the lower flex/ball joint will be replaced with the one rated for this depth which has different rotational stiffness properties as obtained from the website of one subsea flex joint manufacturer.

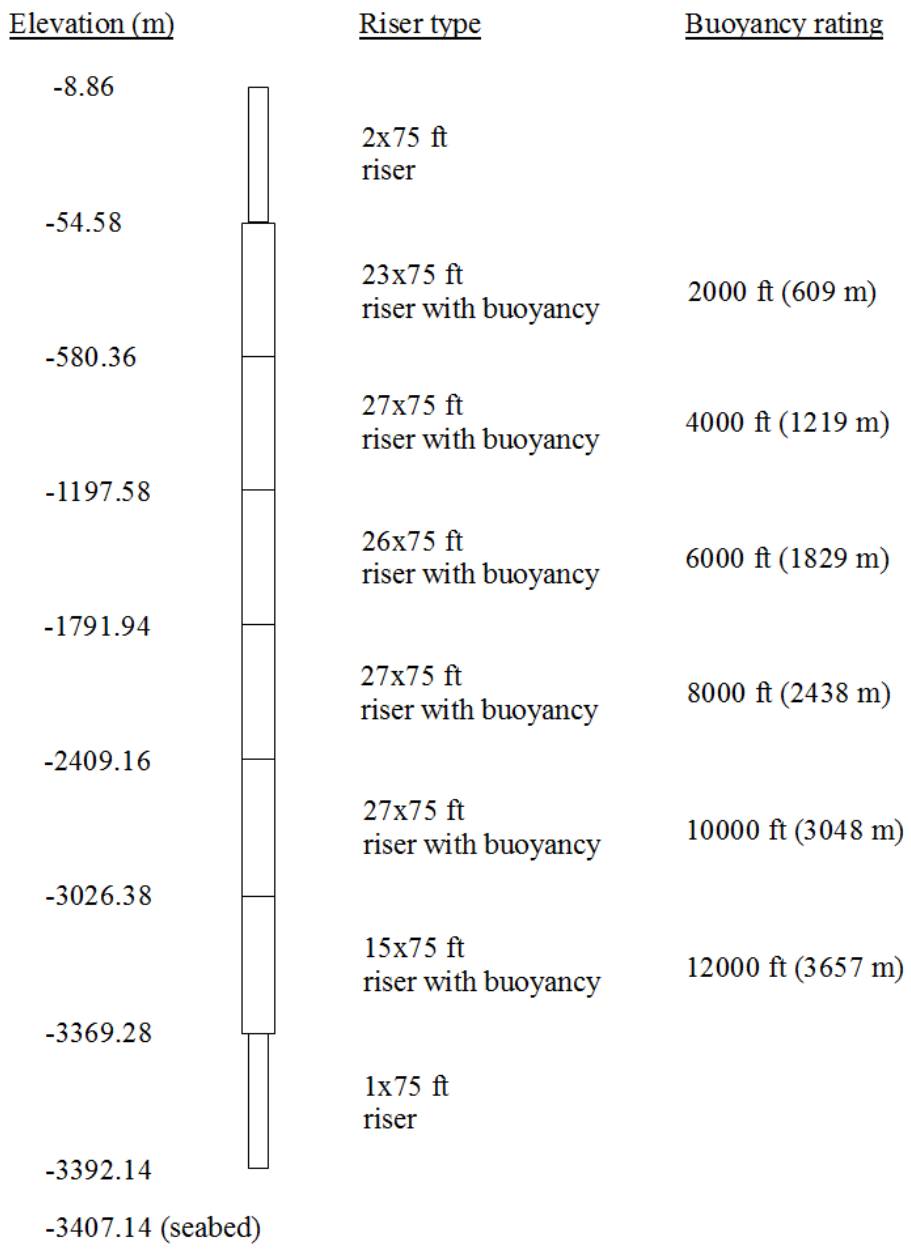

Figure 24. Proposed configuration for 16 inch drilling riser joints.

Due to lack of detailed rotational stiffness data from that manufacturer's website, the stiffness will be assumed as linear and then be used as new input data in Orcaflex for this 16 inch riser case. The manufacturer's data for this flex joint is provided in Table 13.

Type	Working Depth	Max Working Tension	Max Working Pressure	Max Angular Rotation	Rotational Stiffness
Subsea FlexJoint	12000 ft (3657 m)	3000 kips (13349 kN)	6000 psi (41.37 MPa)	$\pm 10^{o}$	94.08 kips.ft/deg (127.6 kNm/deg)

Table 13. Lower flex joint for 16 inch riser (Oil States Industries, 2012).

More detailed properties of the riser joints, buoyancy modules, and auxiliary lines can be seen in the following Table 14 to 16.

Riser Type	Outer Diameter (in)	Inner Diameter (in)	Length/ Joint (m)	Dry Weight (ton)
75 ft bare	16	14.5	22.86	7.63
75 ft + buoyancy (2000 ft)	44	14.5	22.86	14.5
75 ft + buoyancy (4000 ft)	44	14.5	22.86	15.13
75 ft + buoyancy (6000 ft)	44	14.5	22.86	16.06
75 ft + buoyancy (8000 ft)	44	14.5	22.86	17.16
75 ft + buoyancy (10000 ft)	44	14.5	22.86	17.93
75 ft + buoyancy (12000 ft)	44	14.5	22.86	19.17

Table 14. Main riser joint properties for 16 inch riser.

Buoyancy Type	Outer Diameter (in)	Inner Diameter (in)	Service Depth (m)	Net Buoyancy/ Joint (ton)	Material Density (kg/m^3)
Rating 2000 ft	44	16	609	9.21	353
Rating 4000 ft	44	16	1219	8.58	385
Rating 6000 ft	44	16	1829	7.65	433
Rating 8000 ft	44	16	2438	6.55	489
Rating 10000 ft	44	16	3048	5.78	529
Rating 12000 ft	44	16	3657	4.53	593

Table 15. Buoyancy module properties for 16 inch riser.

Auxiliary Line Type	Outer Diameter (in)	Wall Thickness (in)	No. of Lines
Choke & kill line	5	0.625	2 (1 each)
Hydraulic line	3.5	0.25	1
Booster line	4	0.375	1

Table 16. Auxiliary line properties for 16 inch riser.

The grade of the riser is kept the same API 5L X80 with minimum yield stress 555 MPa (80.5 ksi) and minimum tensile strength 625 MPa (90.6 ksi). The weights of riser in Table 14 above are also already including the auxiliary lines which corresponds to Table 16. A 10% of weight contingency was also included to the calculation of weights to accommodate any uncertainties of the riser joint weight.

Buoyancy properties in Table 15 are derived based on same buoyancy density data from the same manufacturer (Cuming Corporation) as for the previous 21 inch riser case. The same 15% of buoyancy loss factor was also included to all calculation of buoyancy modules capacity for this 16 inch riser case. Detailed calculation for all riser and buoyancy module properties including the auxiliary lines can also be found in Appendix C for clarity.

An equivalent line for each riser joints are also created for Orcaflex modelling purpose here. Drag diameter and stress diameter of the equivalent line will be specified according to DNV guideline as described in Subchapter 6-1. For risers with buoyancy attached, the drag diameter will still be taken as the outer diameter of the buoyancy module and for bare risers the drag diameter will be taken as $D + 2\mathrm{d}$ as suggested by the guideline. The values for hydrodynamic coefficients for the slim 16 inch riser will also be taken as recommended by the guideline which is 1.0 as the drag coefficient and 1.1 as the added mass coefficient since the suggested method for determination of drag diameter from the guideline is utilized.

6.3 Environmental conditions

Environmental conditions are very important factor that needs to be carefully applied for the riser analysis as they are the source of hydrodynamic loads on the risers. In an ideal situation, environmental conditions data were obtained from many thorough environmental surveys in a specific area of interest where the operation will be conducted. The area for this work is just fictitious area for conceptual study purpose so there are no any previous environmental data available here. However, after observing environmental conditions and profiles from other areas and referring to some guidelines from standards, a set of environmental data will be compiled for this work. There is assumed that no wind effects to be included in the analysis of this drilling operation. One profile for ocean current speed as a function of depth is randomly selected as given in Table 17 with the maximum speed at the sea surface is 1.0 m/s. This current speed profile will be applied to both 21 inch and 16 inch riser. The current will be applied as flowing in one direction only (i.e. 0^o direction which is from stern to bow of the rig).

Depth (m)	Speed (m/s)
0	1.0
20	0.87
30	0.826
40	0.783
50	0.609
60	0.348
70	0.1
3500	0.1

Table 17. Current speed profiles.

A collection of waves will also be created to be applied to the riser. Again, as no real data were obtained for the wave, a guideline from NORSOK N-003 will be adopted to be used here. The standard mentions that a design wave can be approached to give conservative action effect to structures using a simplified method. The relevant design wave height H_{100}, which corresponds to wave with annual exceedance probability of 10^{-2} (i.e. 100 year wave), may be taken as 1.9

times the significant wave height H_s as obtained from long-run statistics when the sea-state duration is 3 hours (NORSOK, 2007). Still according to the approach in the standard, the wave period to be used in correlation with the calculated design wave height are suggested to be varied within this range:

$$\sqrt{6.5H_{100}} \le T \le \sqrt{11H_{100}}$$

Using the method from NORSOK N-003 as described previously, a range of design wave heights with their corresponding periods can now be defined to represent loadcases that will be applied to the riser. The lack of data for significant wave heights is covered by setting a range of design wave heights. The range will give an approximation about sea-state conditions that might be experienced by the riser during operations.

One point to be added, at some part of the world such as offshore West Africa the wave condition is dominated by swell which can have extreme height and period. According to ISO 19901-1, the swell from distant storms in this region can have long peak periods up to 20 s and can be more. To account for these waves, one additional period of 15 s will be included to illustrate the swell situation. Design periods obtained from NORSOK method will still be used especially for higher frequency waves and for lower frequency they are considered to be accomodated by the swell period.

The waves will be assumed to flow in the same direction as the current, simultaneously (i.e. 0^o direction). Wave theory to be used will be the Dean stream function as suggested by the standard. A set of environmental data is created to obtain a reasonably adequate representation for sea state profiles for analysis and can be seen in Table 18.

Design Wave Height (m)	T1 (s)	T2 (s)	T3 (s)
5	6	7	15
6	7	8	15
7	7	8	15
8	8	9	15
9	8	9	15
10	9	10	15

Table 18. Selected design wave heights and periods for analysis.

6.4 Other considerations

The risers will be analyzed for drilling condition. The required minimum top tension T_{min} as formulated by API RP16Q and ISO 13624-1 (see Subchapter 4.2 and 4.3) will need to be kept lower than the actual top tension in riser at all time during the simulation as suggested by the standards and this is including dynamic effects. To achieve this, a slightly higher top tension will be applied to the riser by the tensioners.

The tensioners installed onboard the drilling rig are known to be approximately 15 m long in full stroke condition. As the tensioners will keep stroking in and out during operation due to wave effects and vessel motions, a safe practice should be implemented which is by setting the mean tensioner stroke to be around the midstroke i.e. 7.5 m. This practice will give the safest range for the tensioners to stroke in and out. A reasonable tolerance will be given for this to accommodate the difficulties in obtaining precise midstroke condition while the required top tension to the riser still needs to be fulfilled. Other benefit from this practice is that it will maintain the inner barrel of the telescopic joints to slip in and out the outer barrel within safe distance.

As stated in the API standard, in case of drift off or drive off occurs it is advised to immediately disconnect the drilling riser from the BOP stack and then suspend it below the rig. Drift off is an unintended lateral movement of a dynamically positioned (DP) vessel away from the intended location which is caused by loss

control in stationkeeping propulsions, while drive off is almost similar with drift off only it is caused by propulsions making mistakes in calculating the required coordinate/distance. To be ready for this condition, some lateral movements (offsets) will be introduced to the rig and to be analyzed as well. The offsets will be measured in terms of percentage relative to water depth.

All simulations in Orcaflex will be done in a total duration of 31 times the corresponding wave period for every case and this is including one wave period of build up stage already. Orcaflex requires at least one wave period for this build up stage duration to help reducing the transient effects. The remaining 30 wave periods for main simulation time is known to be enough for this work to arrive at steady state condition for the simulations considering that a regular wave scenario is used.

Chapter 7
Analysis Result

The proposed riser configurations described in Chapter 6 were analyzed to see the behavior and performance of both 21 inch and 16 inch riser during drilling operation. By applying several different wave heights it will be found out what is the tendency and the limiting metocean condition for each riser to carry out the operation safely at their designated water depth which is 3018 m for the 21 inch riser and 3407.1 m for the 16 inch riser (see Chapter 6).

Comparison between 21 inch and 16 inch riser will be presented here mainly for parameter of interest such as mean and maximum flex/ball joint angle (both upper and lower), Von Mises stress, DNV-OS-F201 Working Stress Design check, dynamic top tension, tensioner dynamic stroke, and dynamic bottom effective tension. These parameters will also be presented on several different vessel offsets to see the effects. Limiting criteria specified in the DNV-OS-F201, API RP 16Q, and ISO 13624-1 Part 1 as described in Chapter 4 will govern the decision and recommendation for the operation.

The mud weight density to be used for comparison is 17 ppg (approximately 2.037 ton/m^3 in metric) and 8.6 ppg (i.e. 1.025 ton/m^3 seawater) which illustrates the heaviest and lightest density range.

Due to height difference between internal drilling fluid column and seawater column outside (riser top elevation is at 28.75 m above sea surface for this specific case), the drilling riser will always experience internal overpressure even when it is filled with seawater. Burst check due to internal overpressure according to DNV-OS-F201 for both risers should be fulfilled and the result can be seen in Table 19 (calculations are given in Appendix A).

Riser Outer Diameter (in)	Wall Thickness (mm)	Drilling Fluid Density (ton/m^3)	Water Depth (m)	Required Wall Thickness (mm)
21	22.22	2.037	3018.0	18.90
16	19.05	2.037	3407.1	16.15

Table 19. Minimum wall thickness for internal overpressure (burst).

The minimum top tension to be applied by setting the six tensioners onboard varies for each riser case. It is basically a function of weight, buoyancy, and internal/external pressure at bottom end of riser. Detailed calculations according to API RP 16Q and ISO 13624-1 Part 1 (see Subchapter 4.2 and 4.3 for reference on this) are given in Appendix D and the result is shown in Table 20 below.

Riser Outer Diameter (in)	Water Depth (m)	Drilling Fluid Density (ton/m^3)	Minimum Top Tension (kN)
21	3018.0	2.037	8849.7
		1.025	414.2
16	3407.1	2.037	5849.3
		1.025	242.2

Table 20. Minimum top tension requirements.

The calculated top tension requirements above are using API buoyancy loss/reduction factor of 1.0. This was selected to avoid utilization of multiple buoyancy loss/reduction factors since a modest loss factor of 15% was already assumed during buoyancy design stage (see Chapter 6).

Based on the minimum top tensions above, a slightly higher tensioner settings are selected to accommodate the dynamic variations which will make the tensioners stroking in/out (retracted/stretched) from midstroke condition (maximum tensioner stroke is 15 m). The tensioner settings are given in Table 21. These settings are maintained constant even when the rig moves from the base location due to offsets.

Riser Outer Diameter (in)	Drilling Fluid Density (ton/m^3)	Tensioner Setting (kN)	No. of Tensioners	Total Tension (kN)
21	2.037	1560	6	9360
	1.025	661		3966
16	2.037	1094		6564
	1.025	501		3006

Table 21. Tensioner settings used for analysis.

The analysis results are presented in Figure A-1 until A-24 and can be found in Appendix E for clarity.

7.1 Discussion on result

The conventional 21 inch and slim 16 inch drilling riser performed well in the analysis and, in fact, gives competitive result to each other. From all results that were presented previously it can be seen immediately that vessel offsets and drilling fluid densities affect all the parameters that need to be satisfied in drilling riser analysis.

Figure A-1 to A-4 show that vessel offset has to be maintained not to move "upstream" or toward the opposite direction of drag (negative offset) excessively since this will cause mean and maximum upper flex/ball joint angles for both risers to quickly exceed the limiting criteria and become worse when using lighter drilling fluid density (8.6 ppg). In contrary, "downstream" vessel offset gives larger mean and maximum lower flex/ball joint angles as can be seen in Figure A-5 to A-8 for both risers which gets even worse when using heavier drilling fluid (17 ppg).

Sufficient top tension will keep the riser in tension all the time and it very much depends on drilling fluid density that is used. It will be less when using lighter drilling fluid and will be more when using heavier drilling fluid. One way to reduce the large angles is by increasing the top tension which, however, will also cause bottom effective tension to increase as well as the axial stress.

The resulted maximum stress in the riser is given in Figure A-9 and A-10. The 16 inch slim riser which has weaker properties (e.g. cross-sectional area for tensile and moment of inertia for bending) than the conventional 21 inch riser, even though both have same pipe grade API X80, has higher stresses in all situations, as expected, and more sensitive with offsets. Since the stresses are already very close to the allowable when using 17 ppg drilling fluid hence it is not a favourable option to increase the top tension because of large riser angles. The fundamental of Von Mises stress is combination of axial, bending, and hoop stress. Working in ultra-deepwater depth using heavy drilling fluid gives huge hoop stress in the risers. That is why choosing other possible option to reduce the angles such as by strictly controlling the vessel offsets is better, and when the situation gets even worse then the riser should be disconnected. Nevertheless, for lighter drilling fluid top tension increase can still be considered as a possible option.

The DNV Working Stress Design check seems to give a satisfactory result as shown in Figure A-11 and A-12. However, this design criteria is to be viewed as plastic Von Mises criteria and is including the effect of strain hardening and wall thinning rather than the traditional yield-elastic Von Mises criteria (see DNV-OS-F201 for further reference). The results are based directly on the time history of the corresponding parameters (see Subchapter 4.1) resulted from the dynamic analysis.

The dynamic top tension results are given in Figure A-13 to A-16. It is known already from Table 20 that when using 8.6 ppg drilling fluid the minimum top tension required is very small for both risers. This means that the combination of riser weight, buoyancy force, and content weight for minimum top tension calculation resulting in a very little "remaining weight" to be lifted by the tensioners. One interesting fact obtained here is that for the 16 inch riser a fourth generation rig having tensioner capacity of 1600 kips (725 ton) will be adequate to do the drilling operation even when using 17 ppg drilling fluid. The minimum top tension is assuming at least one broken tensioner as suggested by the standard. With more number of tensioners available onboard, the amount of minimum top

tension will reduce due to smaller proportion of *N/(N-1)* where *N* is number of tensioners, but this also means more maintenance to be scheduled in the future.

Top tension affects bottom effective tension. From Figure A-17 to A-20 it can be seen that when using lighter drilling fluid the bottom effective tension is larger for both risers and reduces as the heavier fluid are injected even though top tension is increased. Lighter density of drilling fluid gives less hydrostatic internal pressure at any depth compare to the heavier one and it is known already from effective tension concept that internal pressure "reduces" effective tension and external pressure does the opposite (see Subchapter 3.2). To be noticed that LMRP/BOP stack apparent weight was not included in the analysis. The varying bottom effective tension will be carried on to lower flex/ball joint, the stack, and finally to wellhead. The wellhead will then be subjected to tension when the subtraction of LMRP/BOP stack apparent weight to the resulted bottom effective tension is positive. The resulting tension on wellhead can be very high depending on the amount of bottom effective tension. Wellhead fatigue may need to be taken into account as well due to this dynamic loading.

However, optimum design and careful selection of buoyancy module may help reducing criticality of this matter. Overly designed buoyancy helps top tension not to be extremely high when very heavy drilling fluid is considered to be used since the rig tensioner capacity should never be exceeded at anytime during operation but at the same time when lighter drilling fluid is applied the exact same amount of buoyancy will still be there and decreases the gradient/difference between top and bottom effective tension.

Figure A-21 to A-24 provides the dynamic tensioner stroke which its average ideally should be at midstroke position (in this case 7.5 m). For cases with lighter drilling fluid (8.6 ppg) the tensioner is slightly overstroked out hence more top tension need to be set to pull the riser and retract the tensioners back. When this is done, riser angles will be reduced but stresses will increase and, again, bottom effective tension will be higher as well.

Chapter 8
Conclusion

By using the proposed riser configurations for the 21 inch and 16 inch drilling riser previously the analysis results show that for all of the criteria that need to be satisfied the stresses and riser angles are the most critical parameters that become the limiting factor for the operation of both risers, and even more for the 16 inch riser. The drilling mud density also set a barrier for the analysis. Overall, the 21 inch and 16 inch riser are both giving tight and competitive performance which is very interesting to be researched further in the future.

For deepwater application, calm to moderate environment condition with small vessel offset is more favourable situation to conduct drilling operation for both risers since the stresses and angles are closely influenced by this.

Table 22 provides the summary for several properties of the proposed riser configurations for both 21 inch and 16 inch riser at their intended water depths. The 3018 m water depth for the 21 inch riser was selected to illustrate the 10000 ft drilling depth achievement. For the 16 inch riser, the 3407.1 m water depth was obtained after several loops/iterations conducted to achieve approximately close combined stress value (which is maximum at riser bottom due to hoop and axial/tensile stress) with that of the 21 inch riser.

Riser Diameter (in)	Water Depth (m)	No. of Joints	Total Riser Length (m)	Total Riser Dry Weight (ton)	Drilling Fluid Volume (m^3)	Drilling Fluid Weight (ton)	
						8.6 ppg	17 ppg
21	3018.0	131	2994.7	3445.6	664.4	681	1353.4
16	3407.1	148	3383.3	2417.3	442.2	453.3	900.8

Table 22. Summary of riser properties.

It can be seen from Table 22 above that the 16 inch riser, even when operating at water depth more than 10% deeper than the 21 inch riser, gives less total riser dry weight by 29.8% and less total drilling fluid volume by 33.4%. This differences are significantly important especially when a cost-effective alternative solution for drilling operation needs to be examined as more latest generation rigs are under long term contract nowadays.

Fourth generation rig, possibly with less major upgrades/modifications, from Figure A-15 shows enough capability in providing required minimum top tension for the 16 inch riser case using 17 ppg drilling fluid, theoretically. However, a proper full scope of analysis will still be required to be done as the conclusion obtained here was solely based on top tension capacity in this case. Brief capacity comparison for several offshore drilling rigs can be seen in Table 23 below.

Rig Generation	**Rig Name**	**Max Water Depth[1] (m)**	**Variable Deck Load Capacity[1] (ton)**	**Liquid Mud Capacity[1] (m^3)**	**Top Tension Capacity[1] (ton/kips)**	**Day Rate[2] (US$)**
4th	Saipem's Scarabeo 5	2000	3400	380	880/1920	> 400k
5th	Transocean's Sedco Energy	2286	6000	715	1088/2400	> 500k
6th	Odfjell's Deepsea Stavanger	3000	7500	760	1450/3200	> 600k

[1] Obtained from each respective company's website
[2] Day rates are approximated based on article in E&P Magazine, March 19, 2012

Table 23. Several drilling rig capacity comparison.

The fifth and sixth generation rigs have relatively close capacity that is required to drill using 21 inch riser in deepwater areas as can be seen in Table 23 above. The fourth generation rigs with generally almost half VDL (variable deck load) and liquid mud pit capacity will need to "struggle" a lot to achieve the same capability as its newer successors but it still has large opportunity to join the competition for the 16 inch drilling riser case. Regarding this situation a tender-assisted drilling operation can also be viewed as a prospective option for employment of fourth generation rigs.

Bottom effective tension can be an issue as discussed in Subchapter 7.7 when the need to increase top tension emerges. However, when it can be proved that no critical effect may happen on wellhead and the stack due to high tension load then the top tension can be adjusted until desired value for required parameters such as riser angles and tensioner midstroke position is achieved. Further reference on how riser loads will affect the integrity of the stack can be obtained from a paper by Bednar, et al. (1976).

Chapter 9
Future Work Recommendation

The work in this report is a conceptual work which is expected to be able to give an overview on how the 21 inch and 16 drilling riser will perform during drilling operation. Further work on this subject is strongly recommended to be conducted more thoroughly in the future using as minimum assumption as possible and measured/tested data for mechanical properties of riser and buoyancy modules, subsea flex joint stiffness data, and actual range of drilling fluid density to be used.

All weights, including the apparent weight of LMRP/BOP stack, should ideally be obtained from accurate measurement or direct weighing (if possible) to eliminate the needs of unnecessary large safety factor which is actually meant to account for the uncertainties.

Not least important is the environmental condition and metocean data. Site specific information should be gathered prior to conducting all necessary future analysis. All required site surveys may need to be done first when no previous data are available or can not be obtained.

Performing wellhead strength and fatigue analysis may also be required to accompany future works on this subject to be sure that the results in the drilling riser analysis are not giving excessive loading or having critical impact to the wellhead and/or other subsea equipments.

References

ABB Marine, 2012. *Total integration to West Venture - the world's first 5th generation DP drilling rig*. [cited on June 4th, 2012]. Available at: <http://www05.abb.com/global/scot/scot293.nsf/veritydisplay/c1256cc400313660c1256e9e002666eb/$file/west%20venture.pdf>

Almar-Næss, A., 1985. *Fatigue Handbook: Offshore Steel Structures*. Tapir Forlag.

API, 1993. *API RP 16Q Design, Selection, Operation, and Maintenance of Marine Drilling Riser Systems*. American Petroleum Institute.

API, 2007. *API Specification 5L Specification for Line Pipe*. American Petroleum Institute.

Bai, Y. and Bai, Q., 2005. *Subsea Pipelines and Risers*. Elsevier.

Bednar, J. M., Dixon, W. P. and DuMay, W. H., 1976. *Effects of Blowout Preventor End Connections on the Pressure Integrity of a Subsea BOP Stack Under Riser Loads*. In: 1976 Offshore Technology Conference. Houston, Texas 3-6 May 1976. Offshore Technology Conference. OTC 2649.

Boresi, A. P. and Schmidt, R. J., 2003. *Advanced Mechanics of Materials*. 6th ed. John Wiley & Sons.

Case, J., Chilver, L., and Ross, C. T. F., 1999. *Strength of Materials and Structures*. 4th ed. Arnold Publisher.

Childers, M., 2004. *Slim riser an alternate method for deepwater drilling*. Drilling Contractor Magazine, January/February 2004.

Childers, M. and Quintero, A., 2004. *Slim Riser - A Cost-Effective Tool for Ultra Deepwater Drilling*. In: 2004 IADC/SPE Asia Pacific Drilling Technology Conference and Exhibition. Kuala Lumpur, Malaysia 13-15 September 2004. International Association of Drilling Contractors and Society of Petroleum Engineers. IADC/SPE 87982.

Chopra, A. K., 1980. *Dynamics of Structure A Primer*. Earthquake Engineering Research Institute.

Cuming Corporation, 2012. *Catalog 150 C-Float Boyancy Modules for Drilling Risers*. [cited on June 4th, 2012]. Available at: <http://cumingcorp.com/pdf/flotationBRO4-11.pdf>

Dean, R. G. and Dalrymple, R. A., 1991. *Water Wave Mechanics for Engineers and Scientists*. World Scientific.

DNV, 2007. *DNV-OS-F101 Submarine Pipeline Systems*. Det Norske Veritas.

DNV, 2010. *DNV-OS-F201 Dynamic Risers*. Det Norske Veritas.

DNV, 2011. *Wellhead Fatigue Analysis Method*. Det Norske Veritas. [cited on June 4th, 2012]. Available at: <http://www.dnv.com/binaries/wellhead_fatigue_analysis_method_dnv_tcm4-465681.pdf>

E&P Magazine, 2011. *Ultra-deepwater Market Sees More $500,000 Rig Rates*. November 16th, 2011. [cited on June 4th, 2012]. Available at: <http://www.epmag.com/Offshore-Rig-Counts/Ultra-deepwater-Market-Sees-500000-Rig-Rates_91837>

E&P Magazine, 2012. *Down-Market Rigs See Day Rates Rise, New Orders Likely*. March 19th, 2012. [cited on June 4th, 2012]. Available at: <http://www.epmag.com/Production-Drilling/Down-Market-Rigs-Day-Rates-Rise-Orders-Likely_97802>

Euro Asia Energy, 2009. *Company Profiles: Ocean Rig Drilling Deep*. [cited on June 4th, 2012]. Available at: <http://www.euroasiaenergy.com/page/486/Drilling-Deep>

Gudmestad, O. T., 2011. *Lecture notes on Marine Technology spring course at University of Stavanger*. Stavanger.

Harris, L. M., 1972. *An Introduction to Deepwater Floating Drilling Operations*. Tulsa Petroleum Publishing.

ISO, 2005. *ISO 19901-1 Part 1: Metocean design and operating considerations*. International Organization for Standardization.

ISO, 2009. *ISO 13624-1 Part 1: Design and operation of marine drilling riser equipment*. International Organization for Standardization.

Maclachlan, M., 1987. *An Introduction to Marine Drilling*. Oilfield Publications Ltd.

Morison, J. R., O'Brien, M. P., Johnson, J. W. and Schaaf, S. A., 1950. *The Force Exerted by Surface Waves on Piles*. Petroleum Transactions, AIME, Vol. 189.

Mustang Engineering, 2011. *Deepwater Solutions & Records for Concept Selection*. [cited on June 4th, 2012]. Available at: <http://www.mustangeng.com/AboutMustang/Publications/Publications/2011%20Deepwater%20Poster%20Final.pdf>

Nergaard, A., 2012. *Reelwell Drilling Method – Applications on Floaters – A 4000 m WD vision Presentation*. (Obtained from the author directly)

NORSOK, 2007. *NORSOK STANDARD N-003, Action and action effects*. Standard Norge.

Odfjell Drilling, 2012. *Deepsea Stavanger Rig and Riser Specific Data*. (Obtained from the author directly)

Odfjell Drilling, 2012. *Deepsea Stavanger Key Specifications*. [cited on June 4th, 2012]. Available at: <http://www.odfjelldrilling.com/Global/ODFJELL%20OFFSHORE/OUR%20UNITS/OD_teknisk%20spec_DSS_1804.pdf>

Offshore Energy Center, 2000. *Drilling (Mobile Drilling Units) First & Second Generation Semi Submersible Drilling Rigs*. [cited on June 4th, 2012]. Available at: <http://www.oceanstaroec.com/fame/2000/semisubmersible.htm>

Offshore Magazine, 2001. *DRILLING RIG ECONOMICS: Second, third generation semisubmersible drilling fleets positioned for upgrades*. Vol. 61 issue 3. [cited on June 4th, 2012]. Available at: <http://www.offshore-mag.com/articles/print/volume-61/issue-3/news/drilling-rig-economics-second-third-generation-semisubmersible-drilling-fleets-positioned-for-upgrades.html>

Oil Price, 2012. *The Ocean Prospector will Return to Operation after 14 years on the Dock*. May 18th, 2012. [cited on June 4th, 2012]. Available at: <http://oilprice.com/Latest-Energy-News/World-News/The-Ocean-Prospector-will-Return-to-Operation-after-14-years-on-the-Dock.html>

Oil States Industries, 2012. *Subsea FlexJoint Configurations*. [cited on June 4th, 2012]. Available at: <http://www.oilstates.com/fw/main/Subsea-Configurations-375C471.html>

Orcina, 2011. *OrcaFlex Manual Version 9.5a*. Available at: <http://www.orcina.com/SoftwareProducts/OrcaFlex/Documentation/index.php>

Palmer, A. C. and Baldry, J. A. S., 1974. *Lateral Buckling of Axially Constrained Pipelines*. Journal of Petroleum Technology, November 1974.

Palmer, A. C. and King, R. A., 2004. *Subsea Pipeline Engineering*. Pennwell.

Rao, S. S., 2004. *Mechanical Vibrations*. 4th ed. Pearson Prentice Hall.

Sarpkaya, T. and Isaacson, M., 1981. *Mechanics of Wave Forces on Offshore Structures*. Van Nostrand Reinhold.

SEC Info Database, 2002. *Diamond Offshore Drilling Inc*. [cited on June 4th, 2012]. Available at:
<http://www.secinfo.com/dRx61.355.d.htm>

Sheffield, R., 1980. *Floating Drilling : Equipment & Its Use*. Gulf Publishing.

Sparks, C. P., 2007. *Fundamentals of Marine Riser Mechanics: Basic Principles and Simplified Analyses*. PennWell.

Taylor, B., Theiss, D., Toalson, D. and Mowell, R., 2003. *Reducing the Cost of Deepwater Subsea Wells*. In: 2003 Offshore Technology Conference. Houston, Texas 5-8 May 2003. Offshore Technology Conference. OTC 15211.

Theiss, David H., 2003. *Slenderwell Wellhead Benefits and Opportunities of Selected 13" Option*. In: 2003 Offshore Technology Conference. Houston, Texas 5-8 May 2003. Offshore Technology Conference. OTC 15208.

Transocean, 2012. *Our History*. [cited on June 4th, 2012]. Available at:
<http://deepwater.com/fw/main/Our-History-3.html>

Transocean Beacon Magazine, 2011. *Way to GO, Norway!*. Issue 6. [cited on June 4th, 2012]. Available at:
<http://beaconmag.com/Archives/Archive_Spring11/waytogo,norway.html>

Virtual Globe Trotting, 2012. *Ocean Prospector Rig*. [cited on June 4th, 2012]. Available at:
<http://virtualglobetrotting.com/map/offshore-platform-ocean-prospector/view/?service=1>

Wikipedia, 2012. *Bluewater I Rig*. [cited on June 4th, 2012]. Available at:
<http://en.wikipedia.org/wiki/File:Blue_Water_Rig_No._1.JPG>

World Oil, 2005. *New rig designs: Sixth-generation drilling rig is under construction*. Vol. 226, No. 12. [cited on June 4th, 2012]. Available at:
<http://www.worldoil.com/December-2005-New-rig-designs-Sixth-generation-drilling-rig-is-under-construction.html>

Yokokura, K., Nonaka, A. and Takada, M., 1998. *Technical trends of deepwater drilling rig Advancements in drilling equipment & system and in DPS class & reliability presentation of the newest deepwater rig construction "West Future II"*. Journal of the Japanese Association for Petroleum Technology, Vol. 63, No. 5. Available at:
<http://www.japt.org/html/iinkai/drilling/bunkakai/daisuisinn/data/PresenJournal/H10Symposium_Deepwater_Rig_Trend_Survey.pdf>

APPENDIX A
Burst Check Calculation

BURST DNV-OS-F201 (2010) - 21 INCH

Calculation inputs

Outer diameter,	D	=	**21**	in	=	*533,4*	mm	
Specific Minimum Yield Stress,	$SMYS$	=	**555**	MPa	=	*80495,9*	psi	
Specific Minimum Tensile Strength,	$SMTS$	=	**625**	MPa	=	*90648,6*	psi	
Yield stress temperature derating factor,	$f_{y,\,temp}$	=	**0**	MPa	=	*0,0*	psi	
Tensile strength temperature derating factor,	$f_{u,\,temp}$	=	**0**	MPa	=	*0,0*	psi	
Material strength factor,	α_U	=	**0,96**					
Material resistance factor,	γ_m	=	**1,15**					
Safety class resistance factor,	γ_{SC}	=	**1,26**					
Water depth,	d	=	**3018**	m	=	*9901,6*	ft	
Starting elevation of internal fluid,	h_o	=	**28,75**	m				
Internal fluid density,	ρ_i	=	**17**	ppg	=	*2037,1*	kg/m^3	
Seawater density,	ρ_e	=	**1025**	kg/m^3				
Maximum surface design pressure,	p_d	=	**0**	MPa	=	*0,0*	psi	

Calculation outputs

Yield stress,	f_y	$= (SMYS - f_{y,temp}) \cdot \alpha_U$	=	*532,80*	MPa	= *77276,1*	psi
Tensile strength,	f_u	$= (SMTS - f_{u,temp}) \cdot \alpha_U$	=	*600,00*	MPa	= *87022,6*	psi
Height of internal fluid column,	h	$= d + h_o$	=	*3046,75*	m		
Local internal design pressure,	p_{ld}	$= p_d + \rho_i \cdot g \cdot h$	=	*60,89*	MPa	= *8830,7*	psi
Local incidental pressure,	p_{li}	$= p_{ld} + 0.1 \cdot p_d$	=	*60,89*	MPa	= *8830,7*	psi
Local external pressure,	p_e	$= \rho_e \cdot g \cdot h$	=	*30,35*	MPa	= *4401,4*	psi

Minimum required wall thickness without allowances and tolerances, t_1

$$t_1 = \frac{D}{\frac{4}{\sqrt{3}} \cdot \frac{\min\left(f_y ; \frac{f_u}{1.15}\right)}{\gamma_m \gamma_{SC} (p_{li} - p_e)} + 1}$$

= *18,90* mm = *0,744* in

BURST DNV-OS-F201 (2010) - 16 INCH

Calculation inputs

Outer diameter,	D	=	**16**	in	=	*406,4*	mm	
Specific Minimum Yield Stress,	$SMYS$	=	**555**	MPa	=	*80495,9*	psi	
Specific Minimum Tensile Strength,	$SMTS$	=	**625**	MPa	=	*90648,6*	psi	
Yield stress temperature derating factor,	$f_{y,\,temp}$	=	**0**	MPa	=	*0,0*	psi	
Tensile strength temperature derating factor,	$f_{u,\,temp}$	=	**0**	MPa	=	*0,0*	psi	
Material strength factor,	α_U	=	**0,96**					
Material resistance factor,	γ_m	=	**1,15**					
Safety class resistance factor,	γ_{SC}	=	**1,26**					
Water depth,	d	=	**3407,1**	m	=	*11178,1*	ft	
Starting elevation of internal fluid,	h_o	=	**28,75**	m				
Internal fluid density,	ρ_i	=	**17**	ppg	=	*2037,1*	kg/m^3	
Seawater density,	ρ_e	=	**1025**	kg/m^3				
Maximum surface design pressure,	p_d	=	**0**	MPa	=	*0,0*	psi	

Calculation outputs

Yield stress,	f_y	$= (SMYS - f_{y,temp}) \cdot \alpha_U$	=	*532,80*	MPa	= *77276,1*	psi
Tensile strength,	f_u	$= (SMTS - f_{u,temp}) \cdot \alpha_U$	=	*600,00*	MPa	= *87022,6*	psi
Height of internal fluid column,	h	$= d + h_o$	=	*3435,85*	m		
Local internal design pressure,	p_{ld}	$= p_d + \rho_i \cdot g \cdot h$	=	*68,66*	MPa	= *9958,4*	psi
Local incidental pressure,	p_{li}	$= p_{ld} + 0.1 \cdot p_d$	=	*68,66*	MPa	= *9958,4*	psi
Local external pressure,	p_e	$= \rho_e \cdot g \cdot h$	=	*34,26*	MPa	= *4968,9*	psi

Minimum required wall thickness without allowances and tolerances, t_1

$$t_1 = \frac{D}{\frac{4}{\sqrt{3}} \cdot \frac{\min\left(f_y ; \frac{f_u}{1.15}\right)}{\gamma_m \gamma_{SC} (p_{li} - p_e)} + 1}$$

= *16,15* mm = *0,636* in

APPENDIX B
Pipe Properties Calculation

PIPE PROPERTIES - 21 INCH

Calculation inputs

Pipe outer diameter,	D_o	=	**0,533**	m	=	*21*	in
Pipe inner diameter,	D_i	=	**0,489**	m	=	*19,25*	in
Modulus of elasticity,	E	=	**207**	GPa			
Poisson ratio,	v	=	**0,293**				

Calculation outputs

Wall thickness,	WT	=	$\frac{D_o - D_i}{2}$	=	*0,02223*	m	=	*0,875*	in
Cross sectional area,	A_z	=	$\frac{\pi}{4}\left(D_o^2 - D_i^2\right)$	=	*0,03569*	m^2			
Moment of inertia,	I_x	=	$\frac{\pi}{64}\left(D_o^4 - D_i^4\right)$	=	*0,00117*	m^4			
Modulus of rigidity,	G	=	$\frac{E}{2(1+v)}$	=	*80,046*	GPa			
Polar moment of inertia,	J_{zz}	=	$\frac{\pi}{32}\left(D_o^4 - D_i^4\right)$	=	*0,00234*	m^4			
Bending stiffness,	EI_x	=			*241,771*	10^3 kN.m^2			
Axial stiffness,	EA_z	=			*7,388*	10^6 kN			
Torsional stiffness,	GJ_{zz}	=			*186,985*	10^3 kN.m^2			

PIPE PROPERTIES - 16 INCH

Calculation inputs

Pipe outer diameter,	D_o	=	**0,406**	m	=	*16*	in
Pipe inner diameter,	D_i	=	**0,368**	m	=	*14,5*	in
Modulus of elasticity,	E	=	**207**	GPa			
Poisson ratio,	v	=	**0,293**				

Calculation outputs

Wall thickness,	WT	=	$\frac{D_o - D_i}{2}$	=	*0,01905*	m	=	*0,75*	in
Cross sectional area,	A_z	=	$\frac{\pi}{4}\left(D_o^2 - D_i^2\right)$	=	*0,02318*	m^2			
Moment of inertia,	I_x	=	$\frac{\pi}{64}\left(D_o^4 - D_i^4\right)$	=	*0,00044*	m^4			
Modulus of rigidity,	G	=	$\frac{E}{2(1+v)}$	=	*80,046*	GPa			
Polar moment of inertia,	J_{zz}	=	$\frac{\pi}{32}\left(D_o^4 - D_i^4\right)$	=	*0,00087*	m^4			
Bending stiffness,	EI_x	=			*90,217*	10^3 kN.m^2			
Axial stiffness,	EA_z	=			*4,799*	10^6 kN			
Torsional stiffness,	GJ_{zz}	=			*69,773*	10^3 kN.m^2			

APPENDIX C
Riser and Buoyancy Properties Calculation

RISER AND BUOYANCY PROPERTIES - 21 INCH

Length/joint = **22,86** m
Riser material density = **7,85** ton/m^3
Content density = **1,025** ton/m^3 *(changes in content density will not affect geometry and displacements)*
Seawater density = **1,025** ton/m^3

Line Type	Outer Diameter		Wall Thickness		No. of Lines	Inner Diameter		Dry Weight	Content Weight	Submerged & Flooded Weight	Displacement (closed)
	m	in	m	in		m	in	ton/m	ton/m	ton/m	ton/m
Main line	**0,5334**	*21,000*	**0,0222**	*0,875*	**1**	*0,4890*	*19,250*	*0,2802*	*0,1925*	*0,2436*	*0,2290*
Choke/Kill line	**0,1651**	*6,500*	**0,0254**	*1,000*	**2**	*0,1143*	*4,500*	*0,1750*	*0,0210*	*0,1522*	*0,0439*
Booster line	**0,1270**	*5,000*	**0,0127**	*0,500*	**1**	*0,1016*	*4,000*	*0,0358*	*0,0083*	*0,0311*	*0,0130*
Hydraulic line	**0,0732**	*2,882*	**0,0071**	*0,280*	**2**	*0,0590*	*2,322*	*0,0232*	*0,0056*	*0,0202*	*0,0086*
Equivalent line	*0,6049*	*23,814*	*0,0367*	*1,445*	*1*	*0,5315*	*20,925*	*0,5142*	*0,2274*	*0,4470*	*0,2945*

Buoyancy Type	Outer Diameter		Inner Diameter		Buoy Density	Buoy Dry Weight	Buoy Displacement	Efficiency Factor	Net Buoy Displacement
	m	in	m	in	ton/m^3	ton/m	ton/m		ton/m
Rating 2000 ft	**1,4224**	*56,000*	*0,5334*	*21,000*	**0,353**	*0,4821*	*1,3342*	**0,85**	*1,1341*
Rating 4000 ft	*1,4224*	*56,000*	*0,5334*	*21,000*	**0,385**	*0,5257*	*1,3342*	*0,85*	*1,1341*
Rating 6000 ft	*1,4224*	*56,000*	*0,5334*	*21,000*	**0,433**	*0,5913*	*1,3342*	*0,85*	*1,1341*
Rating 8000 ft	*1,4224*	*56,000*	*0,5334*	*21,000*	**0,489**	*0,6684*	*1,3342*	*0,85*	*1,1341*
Rating 10000 ft	*1,4224*	*56,000*	*0,5334*	*21,000*	**0,529**	*0,7224*	*1,3342*	*0,85*	*1,1341*

Input for Orcaflex

Riser weight contingency = **10** %

Line Type	OD (geometry)		ID (geometry)		OD (drag)		Dry Weight		Submerged & Flooded Weight		Displacement (closed)		Net Uplift by Buoy	
	m	in	m	in	m	in	ton	ton/m	ton	ton/m	ton	ton/m	ton	ton/m
75 ft riser	*0,6117*	*24,084*	*0,5315*	*20,925*	*0,8636*	*34,000*	*12,9295*	*0,5656*	*11,2413*	*0,4917*	*6,8868*	*0,3013*	*0*	*0*
75 ft riser + buoyancy rating 2000 ft	*1,3322*	*52,447*	*0,5315*	*20,925*	*1,4224*	*56,000*	*23,9492*	*1,0476*	*-3,5109*	*-0,1536*	*32,659*	*1,4286*	*14,752*	*0,6453*
75 ft riser + buoyancy rating 4000 ft	*1,3322*	*52,447*	*0,5315*	*20,925*	*1,4224*	*56,000*	*24,9481*	*1,0913*	*-2,5119*	*-0,1099*	*32,659*	*1,4286*	*13,753*	*0,6016*
75 ft riser + buoyancy rating 6000 ft	*1,3322*	*52,447*	*0,5315*	*20,925*	*1,4224*	*56,000*	*26,4466*	*1,1569*	*-1,0135*	*-0,0443*	*32,659*	*1,4286*	*12,255*	*0,5361*
75 ft riser + buoyancy rating 8000 ft	*1,3322*	*52,447*	*0,5315*	*20,925*	*1,4224*	*56,000*	*28,2094*	*1,2340*	*0,7493*	*0,0328*	*32,659*	*1,4286*	*10,492*	*0,4590*
75 ft riser + buoyancy rating 10000 ft	*1,3322*	*52,447*	*0,5315*	*20,925*	*1,4224*	*56,000*	*29,4434*	*1,2880*	*1,9834*	*0,0868*	*32,659*	*1,4286*	*9,258*	*0,4050*

RISER AND BUOYANCY PROPERTIES - 16 INCH

Length/joint = **22,86** m
Riser material density = **7,85** ton/m^3
Content density = **1,025** ton/m^3 *(changes in content density will not affect geometry and displacements)*
Seawater density = **1,025** ton/m^3

Line Type	Outer Diameter		Wall Thickness		No. of Lines	Inner Diameter		Dry Weight	Content Weight	Submerged & Flooded Weight	Displacement (closed)
	m	in	m	in		m	in	ton/m	ton/m	ton/m	ton/m
Main line	**0,4064**	*16,000*	**0,0191**	*0,750*	**1**	*0,3683*	*14,500*	*0,1820*	*0,1092*	*0,1582*	*0,1330*
Choke/Kill line	**0,1270**	*5,000*	**0,0159**	*0,625*	**2**	*0,0953*	*3,750*	*0,0870*	*0,0146*	*0,0757*	*0,0260*
Booster line	**0,1016**	*4,000*	**0,0095**	*0,375*	**1**	*0,0826*	*3,250*	*0,0216*	*0,0055*	*0,0188*	*0,0083*
Hydraulic line	**0,0889**	*3,500*	**0,0064**	*0,250*	**1**	*0,0762*	*3,000*	*0,0129*	*0,0047*	*0,0112*	*0,0064*
Equivalent line	*0,4644*	*18,283*	*0,0282*	*1,111*	*1*	*0,4079*	*16,060*	*0,3035*	*0,1340*	*0,2639*	*0,1736*

Buoyancy Type	Outer Diameter		Inner Diameter		Buoy Density	Buoy Dry Weight	Buoy Displacement	Efficiency Factor	Net Buoy Displacement
	m	in	m	in	ton/m^3	ton/m	ton/m		ton/m
Rating 2000 ft	**1,1176**	*44,000*	*0,4064*	*16,000*	**0,353**	*0,3005*	*0,8319*	**0,85**	*0,7071*
Rating 4000 ft	*1,1176*	*44,000*	*0,4064*	*16,000*	**0,385**	*0,3277*	*0,8319*	*0,85*	*0,7071*
Rating 6000 ft	*1,1176*	*44,000*	*0,4064*	*16,000*	**0,433**	*0,3686*	*0,8319*	*0,85*	*0,7071*
Rating 8000 ft	*1,1176*	*44,000*	*0,4064*	*16,000*	**0,489**	*0,4167*	*0,8319*	*0,85*	*0,7071*
Rating 10000 ft	*1,1176*	*44,000*	*0,4064*	*16,000*	**0,529**	*0,4503*	*0,8319*	*0,85*	*0,7071*
Rating 12000 ft	*1,1176*	*44,000*	*0,4064*	*16,000*	**0,593**	*0,5048*	*0,8319*	*0,85*	*0,7071*

Input for Orcaflex

Riser weight contingency = **10** %

Line Type	OD (geometry)		ID (geometry)		OD (drag)		Dry Weight		Submerged & Flooded Weight		Displacement (closed)		Net Uplift by Buoy	
	m	in	m	in	m	in	ton	ton/m	ton	ton/m	ton	ton/m	ton	ton/m
75 ft riser	*0,4696*	*18,490*	*0,4079*	*16,060*	*0,6604*	*26,000*	*7,6330*	*0,3339*	*6,6363*	*0,2903*	*4,0591*	*0,1776*	*0*	*0*
75 ft riser + buoyancy rating 2000 ft	*1,0460*	*41,179*	*0,4079*	*16,060*	*1,1176*	*44,000*	*14,5024*	*0,6344*	*-2,5686*	*-0,1124*	*20,133*	*0,8807*	*9,205*	*0,4027*
75 ft riser + buoyancy rating 4000 ft	*1,0460*	*41,179*	*0,4079*	*16,060*	*1,1176*	*44,000*	*15,1251*	*0,6616*	*-1,9459*	*-0,0851*	*20,133*	*0,8807*	*8,582*	*0,3754*
75 ft riser + buoyancy rating 6000 ft	*1,0460*	*41,179*	*0,4079*	*16,060*	*1,1176*	*44,000*	*16,0592*	*0,7025*	*-1,0118*	*-0,0443*	*20,133*	*0,8807*	*7,648*	*0,3346*
75 ft riser + buoyancy rating 8000 ft	*1,0460*	*41,179*	*0,4079*	*16,060*	*1,1176*	*44,000*	*17,1581*	*0,7506*	*0,0871*	*0,0038*	*20,133*	*0,8807*	*6,549*	*0,2865*
75 ft riser + buoyancy rating 10000 ft	*1,0460*	*41,179*	*0,4079*	*16,060*	*1,1176*	*44,000*	*17,9273*	*0,7842*	*0,8564*	*0,0375*	*20,133*	*0,8807*	*5,780*	*0,2528*
75 ft riser + buoyancy rating 12000 ft	*1,0460*	*41,179*	*0,4079*	*16,060*	*1,1176*	*44,000*	*19,1728*	*0,8387*	*2,1018*	*0,0919*	*20,133*	*0,8807*	*4,534*	*0,1984*

APPENDIX D
Minimum Top Tension Calculation

MINIMUM TOP TENSION CALCULATION API RP 16Q (1993) - 21 INCH

Length/joint =	**22,86**	m
Starting elevation of internal fluid =	**28,75**	m
Elevation of last riser end =	**-3003,02**	m
Riser material density, ρ_s =	**7,85**	ton/m^3
Seawater density, ρ_w =	**1,025**	ton/m^3
Submerged weight tolerance factor, f_{wt} =	**1,05**	
Buoyancy loss and tolerance factor, f_{bt} =	**1**	
No. of tensioners, N =	**6**	
No. of tensioners subject to sudden failure, n =	**1**	
Reduction factor relating vertical tension, R_f =	**0,95**	*(0,95 for drilling; 0,9 for non-drilling)*

Properties	75 ft riser	75 ft riser + buoyancy rating 2000 ft	75 ft riser + buoyancy rating 4000 ft	75 ft riser + buoyancy rating 6000 ft	75 ft riser + buoyancy rating 8000 ft	75 ft riser + buoyancy rating 10000 ft	
Main pipe OD geometry (m)	**0,6117**	*0,6117*	*0,6117*	*0,6117*	*0,6117*	*0,6117*	
Main pipe ID geometry (m)	**0,5315**	*0,5315*	*0,5315*	*0,5315*	*0,5315*	*0,5315*	
Main pipe submerged weight, W_s (ton)	*11,242*	*11,242*	*11,242*	*11,242*	*11,242*	*11,242*	
Net uplift by buoy, B_n (ton)	*0*	**14,752**	**13,753**	**12,255**	**10,492**	**9,258**	

Line Type	No. of joints	W_s/joint (ton)	W_s (ton)	$W_s \cdot f_{wt}$ (ton)	B_n/joint (ton)	B_n (ton)	$B_n \cdot f_{bt}$ (ton)
Slip joint outer barrel w/o aux. lines (weight in air)*	*1*	*17,686*	*17,686*	*18,570*	*0*	*0*	*0*
Slip joint outer barrel w/ aux. lines (weight in air)*	*1*	*8,595*	*8,595*	*9,025*	*0*	*0*	*0*
75 ft riser	**3**	*11,242*	*33,725*	*35,411*	*0*	*0*	*0*
75 ft riser + buoyancy rating 2000 ft	**23**	*11,242*	*258,557*	*271,485*	*14,752*	*339,296*	*339,296*
75 ft riser + buoyancy rating 4000 ft	**27**	*11,242*	*303,524*	*318,700*	*13,753*	*371,331*	*371,331*
75 ft riser + buoyancy rating 6000 ft	**27**	*11,242*	*303,524*	*318,700*	*12,255*	*330,885*	*330,885*
75 ft riser + buoyancy rating 8000 ft	**27**	*11,242*	*303,524*	*318,700*	*10,492*	*283,284*	*283,284*
75 ft riser + buoyancy rating 10000 ft	**24**	*11,242*	*269,799*	*283,289*	*9,258*	*222,192*	*222,192*
**Data from Odfjell Drilling (2012)*			Total =	*1573,879*		Total =	*1546,988*

Parameters	Internal fluid density, ρ_m (ppg)	
	8,554	**17**
Internal fluid column height, H_m (m)	*3031,77*	*3031,77*
Seawater column height, H_w (m)	*3003,02*	*3003,02*
Inner cross-sectional area of riser, A_i (m^2)	*0,22186*	*0,22186*
Internal fluid pressure, $\rho_m \cdot g \cdot H_m$ (kN/m^2)	*30485,1*	*60585,2*
Seawater pressure, $\rho_w \cdot g \cdot H_w$ (kN/m^2)	*30196,1*	*30196,1*
Minimum slip ring tension, T_{SRmin} (kN)	*327,91*	*7006,05*
Minimum top tension, T_{min} (kN)	*414,21*	*8849,74*

MINIMUM TOP TENSION CALCULATION API RP 16Q (1993) - 16 INCH

Length/joint =	**22,86**	m
Starting elevation of internal fluid =	**28,75**	m
Elevation of last riser end =	**-3392,14**	m
Riser material density, ρ_s =	**7,85**	ton/m^3
Seawater density, ρ_w =	**1,025**	ton/m^3
Submerged weight tolerance factor, f_{wt} =	**1,05**	
Buoyancy loss and tolerance factor, f_{bt} =	**1**	
No. of tensioners, N =	**6**	
No. of tensioners subject to sudden failure, n =	**1**	
Reduction factor relating vertical tension, R_f =	**0,95**	*(0,95 for drilling; 0,9 for non-drilling)*

Properties	75 ft riser	75 ft riser + buoyancy rating 2000 ft	75 ft riser + buoyancy rating 4000 ft	75 ft riser + buoyancy rating 6000 ft	75 ft riser + buoyancy rating 8000 ft	75 ft riser + buoyancy rating 10000 ft	75 ft riser + buoyancy rating 12000 ft
Main pipe OD geometry (m)	**0,4696**	*0,4696*	*0,4696*	*0,4696*	*0,4696*	*0,4696*	*0,4696*
Main pipe ID geometry (m)	**0,4079**	*0,4079*	*0,4079*	*0,4079*	*0,4079*	*0,4079*	*0,4079*
Main pipe submerged weight, W_s (ton)	*6,636*	*6,636*	*6,636*	*6,636*	*6,636*	*6,636*	*6,636*
Net uplift by buoy, B_n (ton)	*0*	**9,205**	**8,582**	**7,648**	**6,549**	**5,780**	**4,534**

Line Type	No. of joints	W_s/joint (ton)	W_s (ton)	$W_s \cdot f_{wt}$ (ton)	B_n/joint (ton)	B_n (ton)	$B_n \cdot f_{bt}$ (ton)
Slip joint outer barrel w/o aux. lines (weight in air)*	*1*	*17,686*	*17,686*	*18,570*	*0*	*0*	*0*
Slip joint outer barrel w/ aux. lines (weight in air)*	*1*	*8,595*	*8,595*	*9,025*	*0*	*0*	*0*
75 ft riser	**3**	*6,636*	*19,909*	*20,904*	*0*	*0*	*0*
75 ft riser + buoyancy rating 2000 ft	**23**	*6,636*	*152,635*	*160,267*	*9,205*	*211,712*	*211,712*
75 ft riser + buoyancy rating 4000 ft	**27**	*6,636*	*179,180*	*188,139*	*8,582*	*231,718*	*231,718*
75 ft riser + buoyancy rating 6000 ft	**26**	*6,636*	*172,544*	*181,171*	*7,648*	*198,850*	*198,850*
75 ft riser + buoyancy rating 8000 ft	**27**	*6,636*	*179,180*	*188,139*	*6,549*	*176,828*	*176,828*
75 ft riser + buoyancy rating 10000 ft	**27**	*6,636*	*179,180*	*188,139*	*5,780*	*156,057*	*156,057*
75 ft riser + buoyancy rating 12000 ft	**15**	*6,636*	*99,545*	*104,522*	*4,534*	*68,017*	*68,017*
			Total =	*1058,877*		Total =	*1043,183*

**Data from Odfjell Drilling (2012)*

Parameters	Internal fluid density, ρ_m (ppg)	
	8,554	**17**
Internal fluid column height, H_m (m)	*3420,89*	*3420,89*
Seawater column height, H_w (m)	*3392,14*	*3392,14*
Inner cross-sectional area of riser, A_i (m^2)	*0,1307*	*0,1307*
Internal fluid pressure, $\rho_m \cdot g \cdot H_m$ (kN/m^2)	*34397,7*	*68361,2*
Seawater pressure, $\rho_w \cdot g \cdot H_w$ (kN/m^2)	*34108,8*	*34108,8*
Minimum slip ring tension, T_{SRmin} (kN)	*191,72*	*4630,72*
Minimum top tension, T_{min} (kN)	*242,18*	*5849,34*

APPENDIX E
Analysis Result

E.1 Flex/ball joint angle dynamic results

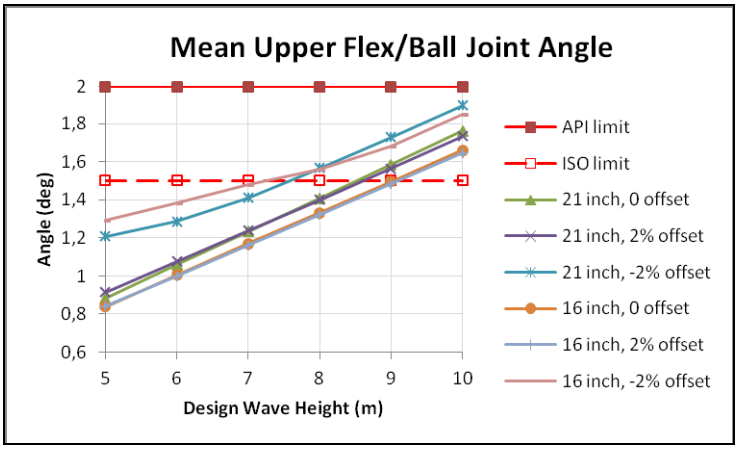

Figure A-1. Mean upper flex/ball joint angle (17 ppg mud).

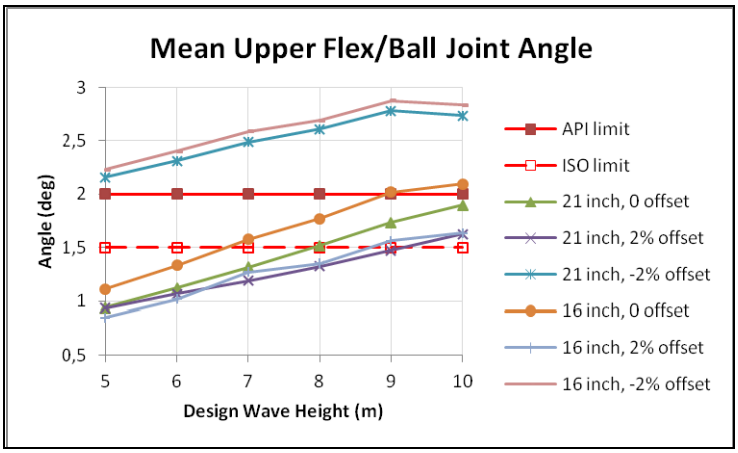

Figure A-2. Mean upper flex/ball joint angle (8.6 ppg mud).

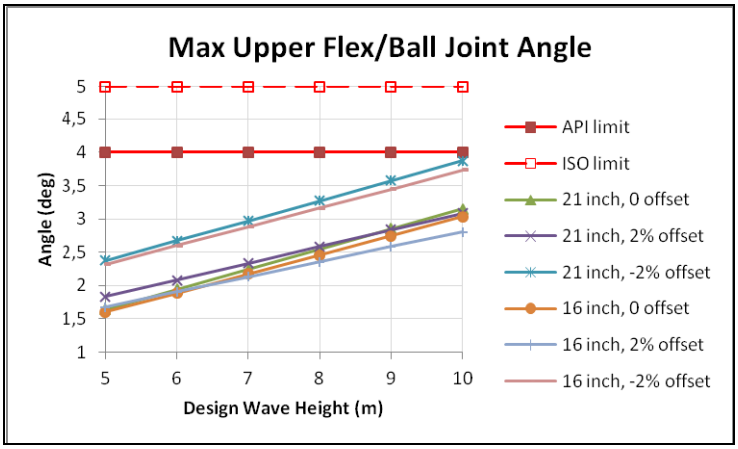

Figure A-3. Maximum upper flex/ball joint angle (17 ppg mud).

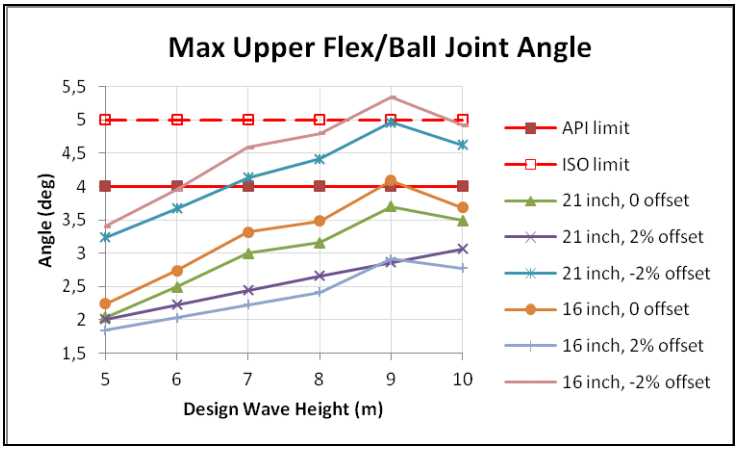

Figure A-4. Maximum upper flex/ball joint angle (8.6 ppg mud).

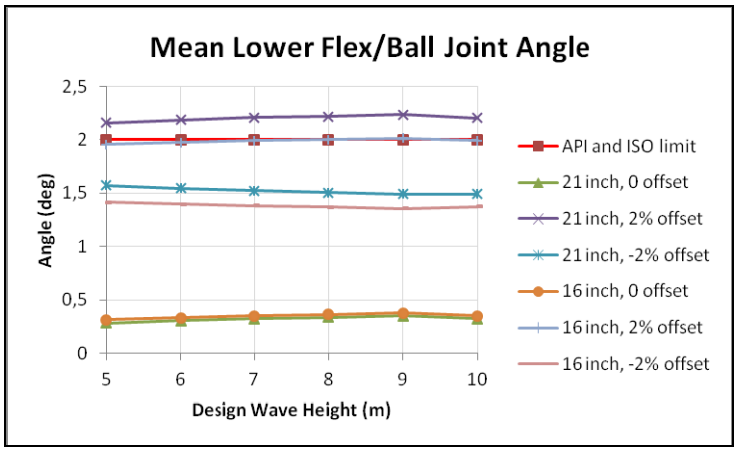

Figure A-5. Mean lower flex/ball joint angle (17 ppg mud).

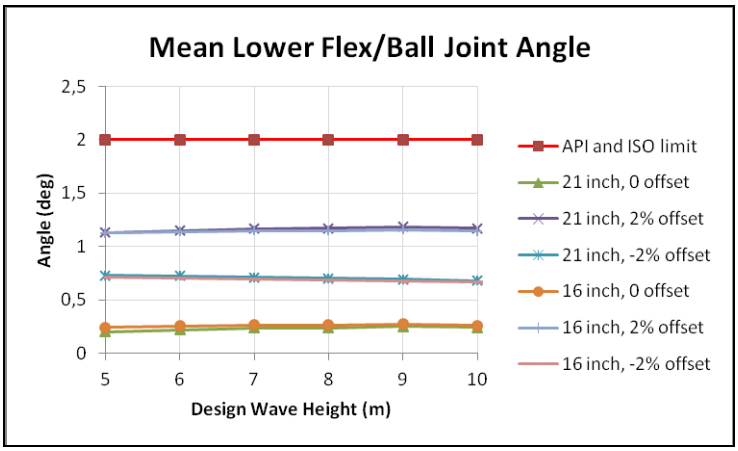

Figure A-6. Mean lower flex/ball joint angle (8.6 ppg mud).

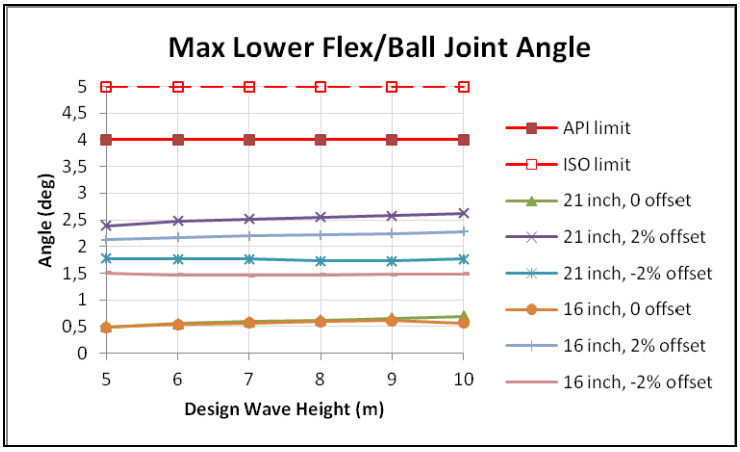

Figure A-7. Maximum lower flex/ball joint angle (17 ppg mud).

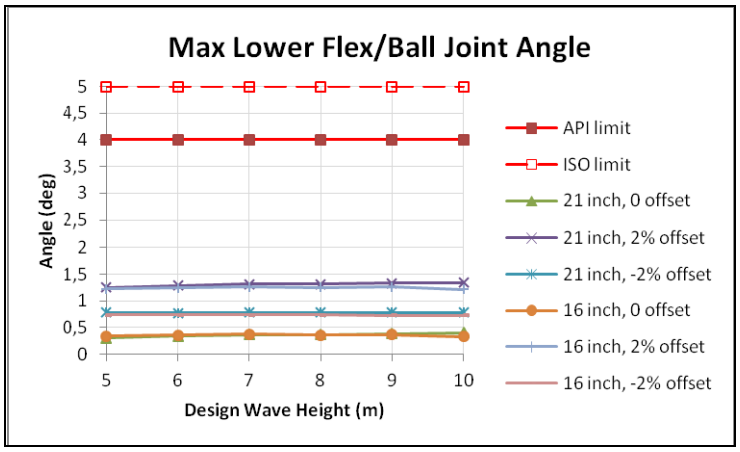

Figure A-8. Maximum lower flex/ball joint angle (8.6 ppg mud).

E.2 Von Mises stress dynamic results

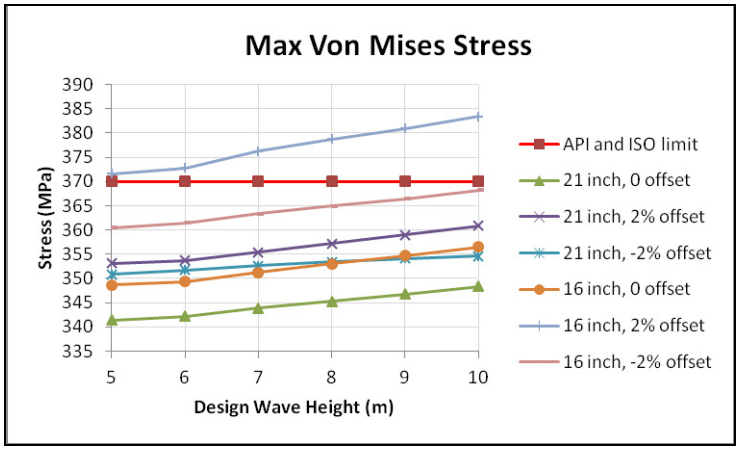

Figure A-9. Maximum Von Mises stress (17 ppg mud).

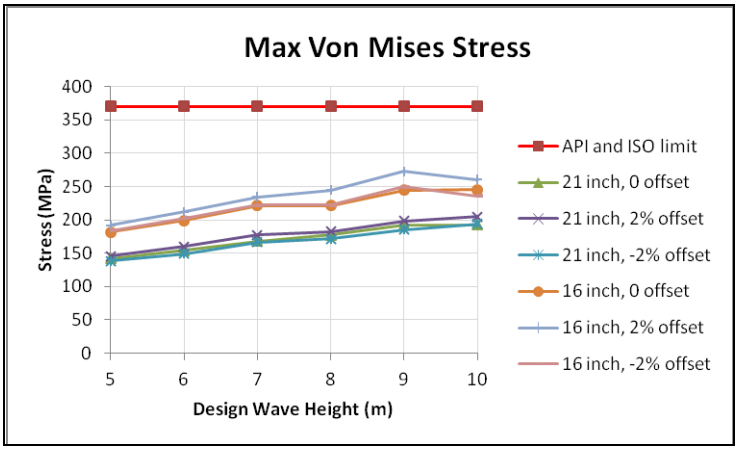

Figure A-10. Maximum Von Mises stress (8.6 ppg mud).

E.3 DNV-OS-F201 WSD check dynamic results

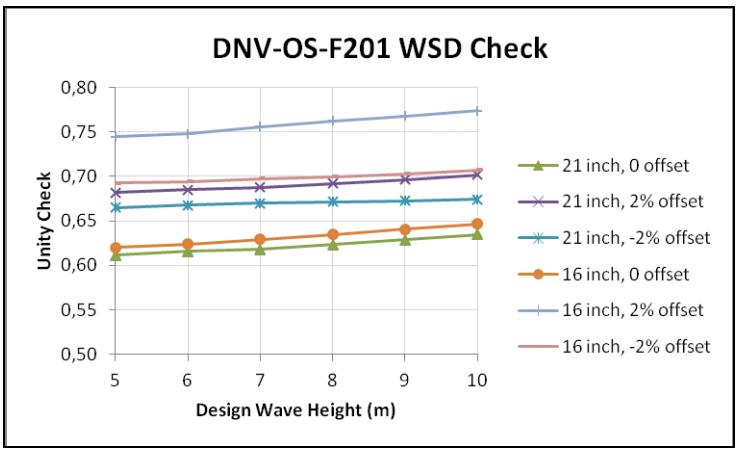

Figure A-11. DNV-OS-F201 WSD unity check (17 ppg mud).

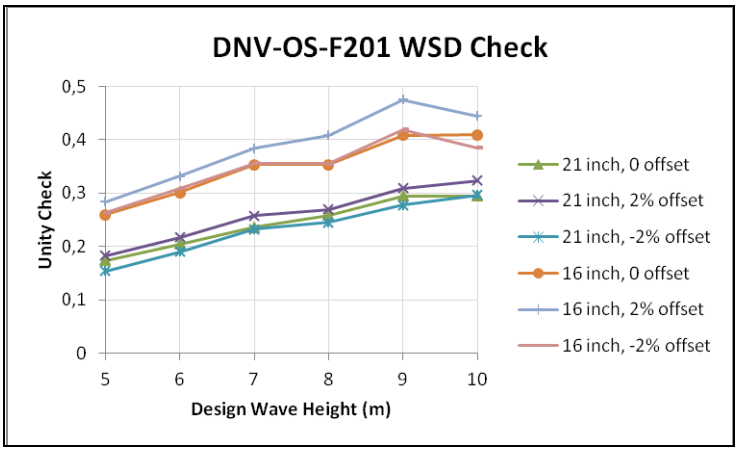

Figure A-12. DNV-OS-F201 WSD unity check (8.6 ppg mud).

E.4 Dynamic top tension results

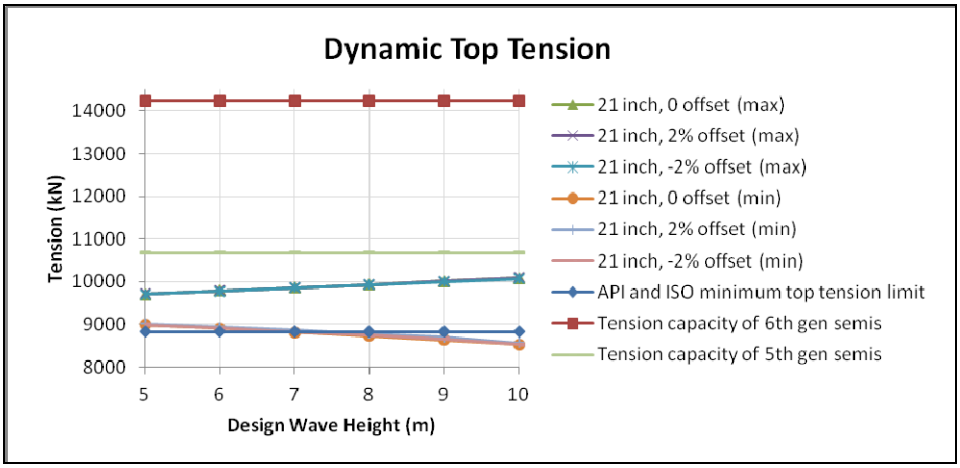

Figure A-13. 21 inch riser dynamic top tension (17 ppg mud).

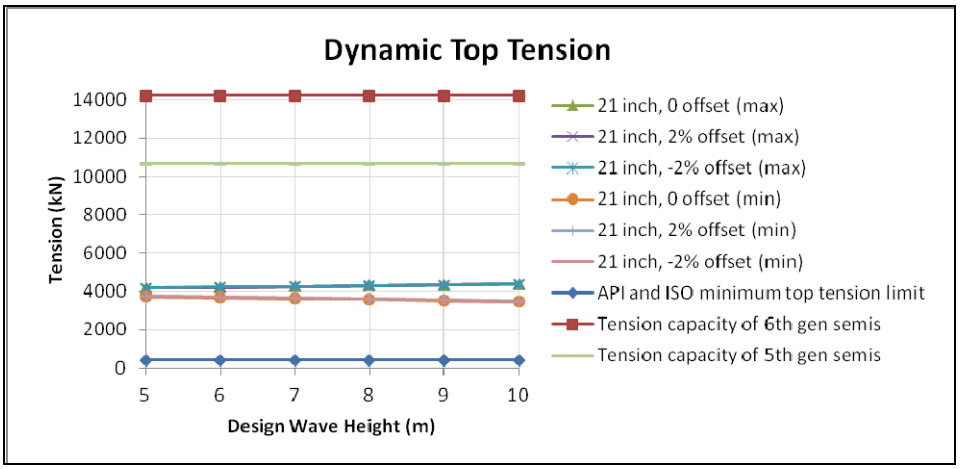

Figure A-14. 21 inch riser dynamic top tension (8.6 ppg mud).

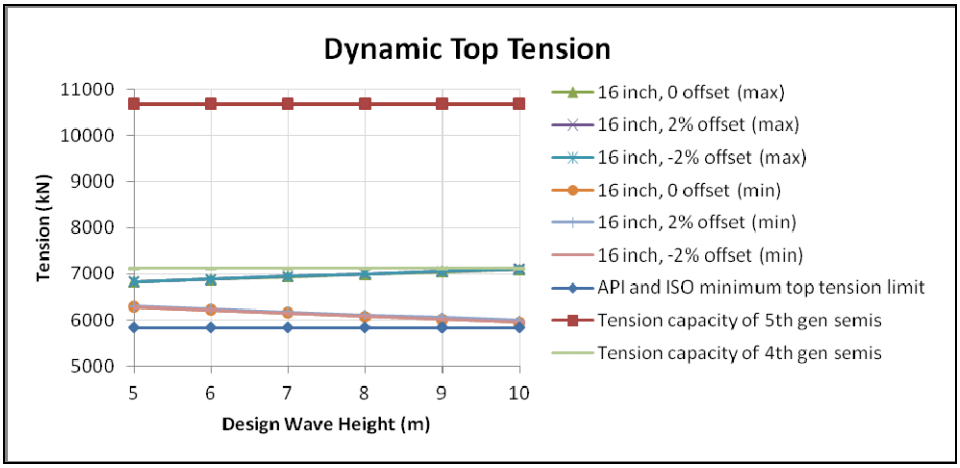

Figure A-15. 16 inch riser dynamic top tension (17 ppg mud).

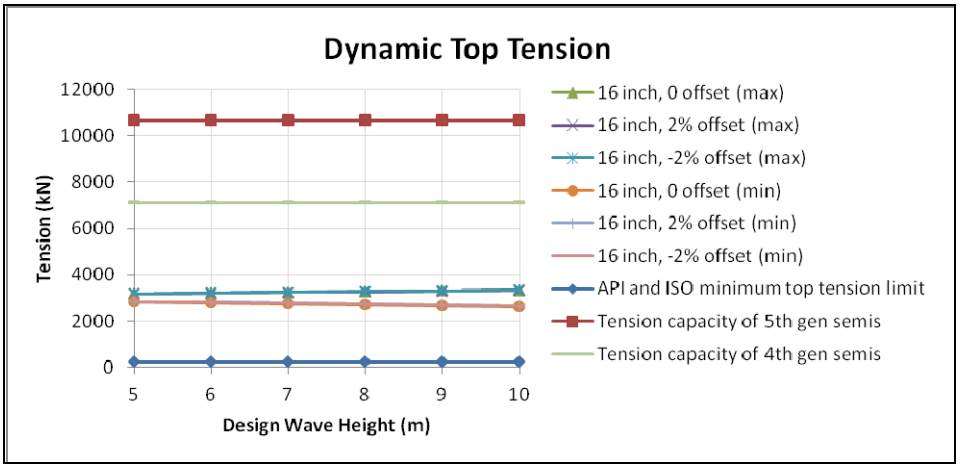

Figure A-16. 16 inch riser dynamic top tension (8.6 ppg mud).

E.5 Bottom effective tension dynamic results

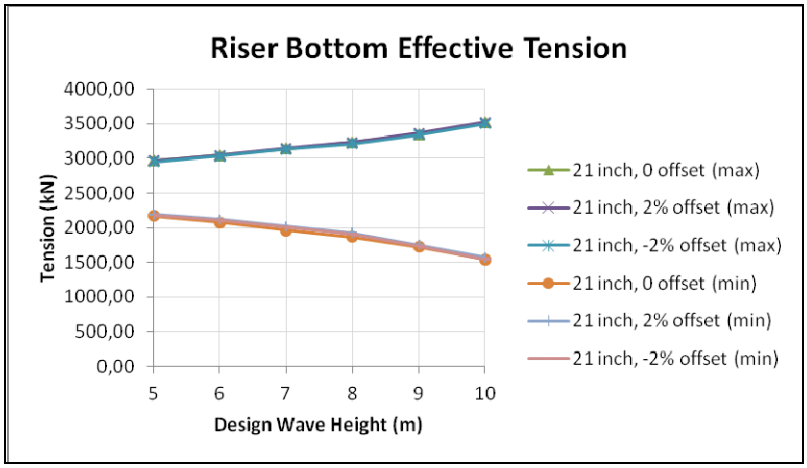

Figure A-17. 21 inch riser dynamic bottom effective tension (17 ppg mud).

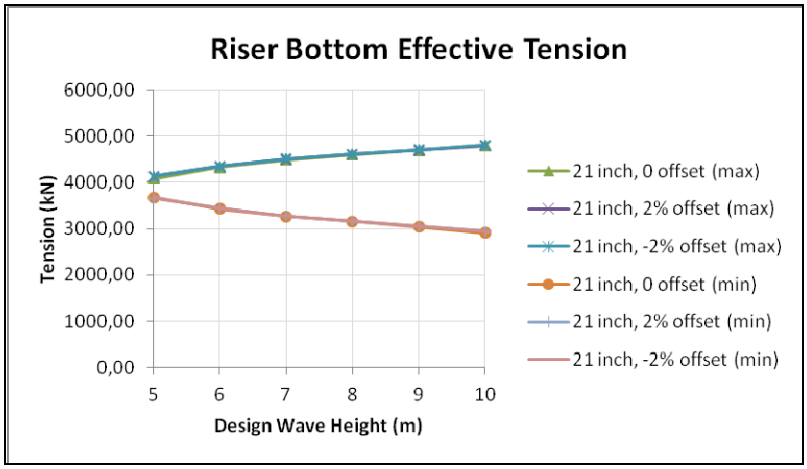

Figure A-18. 21 inch riser dynamic bottom effective tension (8.6 ppg mud).

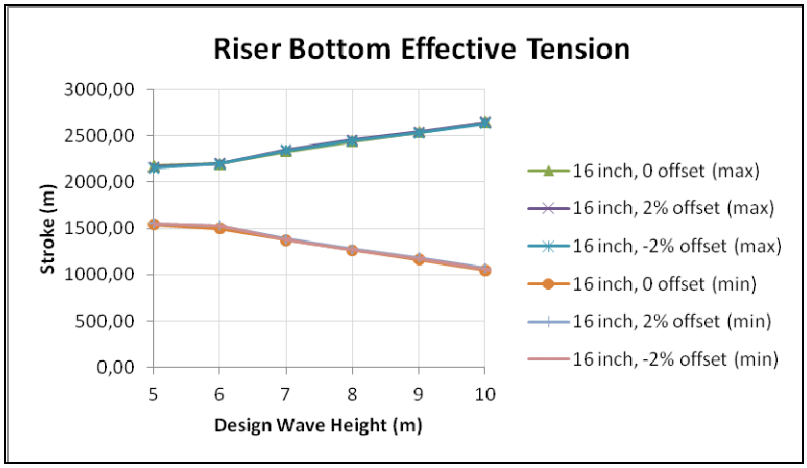

Figure A-19. 16 inch riser dynamic bottom effective tension (17 ppg mud).

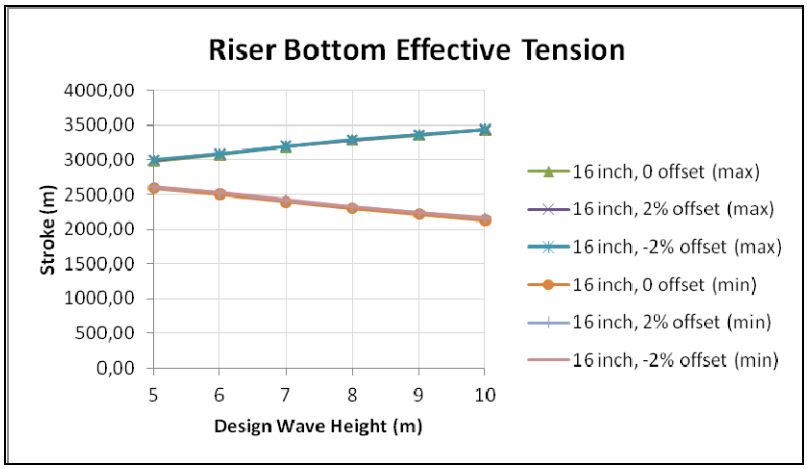

Figure A-20. 16 inch riser dynamic bottom effective tension (8.6 ppg mud).

E.6 Tensioner stroke dynamic results

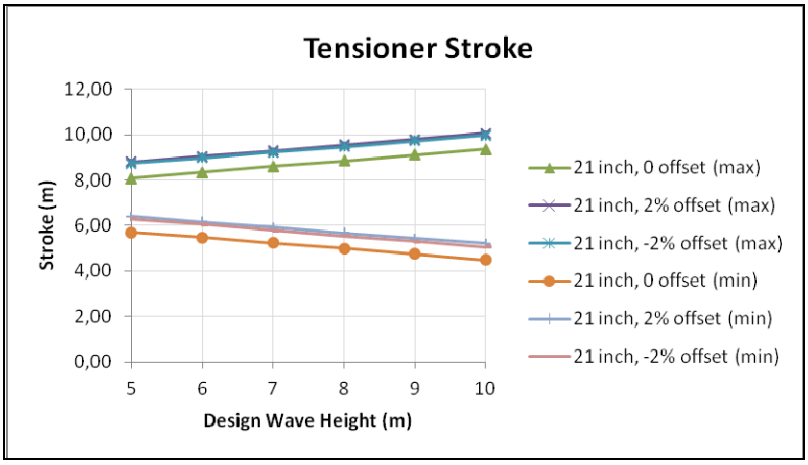

Figure A-21. 21 inch riser dynamic tensioner stroke (17 ppg mud).

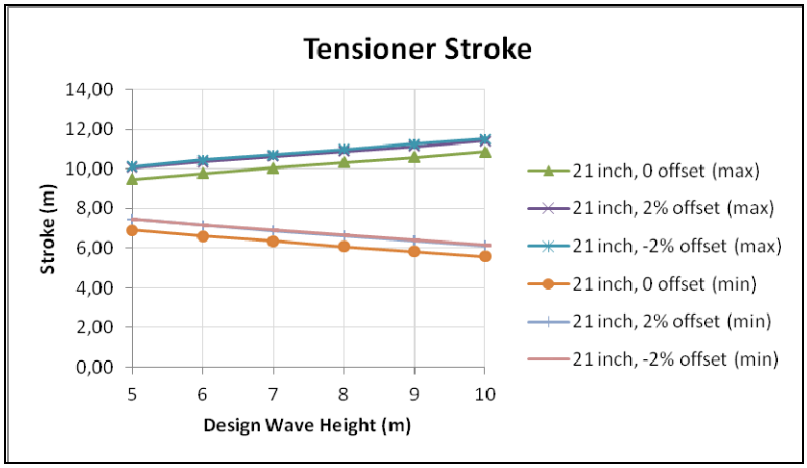

Figure A-22. 21 inch riser dynamic tensioner stroke (8.6 ppg mud).

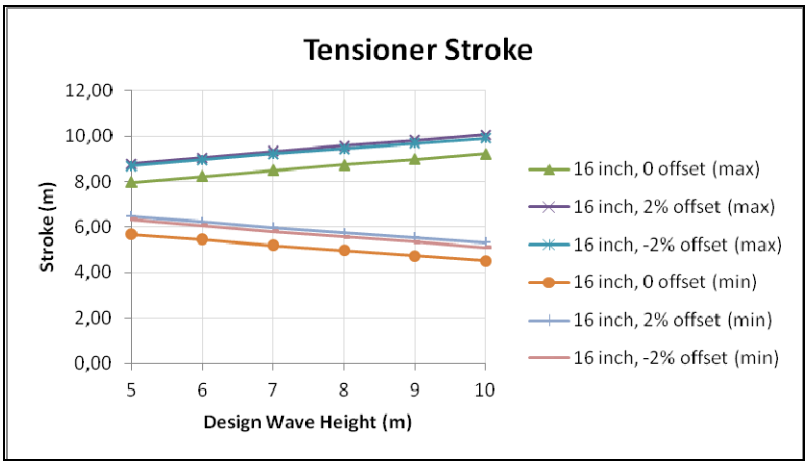

Figure A-23. 16 inch riser dynamic tensioner stroke (17 ppg mud).

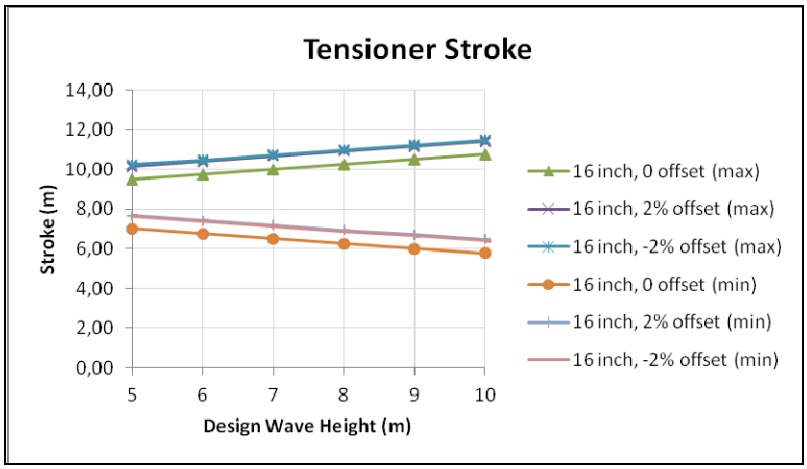

Figure A-24. 16 inch riser dynamic tensioner stroke (8.6 ppg mud).